

THE COMPLETE SET OF JITTERBUG TRANSFORMERS AND THE ANALYSIS OF THEIR MOTION

H. F. VERHEYEN

De Reep, 19, 2230 Schilde, Belgium

Abstract—During many decades and in different locations people have been fascinated with the remarkable variety of ideas and inventions of Richard Buckminster Fuller. Some admire him highly for his versatility while others despise him for not having been a well-outlined architect, engineer or mathematician. And yet in any field his genius revealed itself in original concepts so many in number, that hardly any of these could have been fully worked out during his lifetime. Among these is the Jitterbug, by many considered merely as a geometrical gadget with no further use than performing an attractive transformation between some polyhedra. However, the Jitterbug inspired others to establish similar transformations between some more polyhedra, and there have been publications on these. In these transformations, one could observe Jitterbug-like structures, although they were not studied as sets on their own, but merely appearing while one polyhedron transforms into another one. Clearly there must exist a number of Jitterbug-like transformers and this number must be found when an appropriate definition is applied within the groups of symmetry.

This opens a whole field of investigation one can compare with the study of uniform polyhedra during its history. Since the previous century many new discoveries had been made, but not until 1954 was this matter mathematically dealt with, and in a way that the entire number of uniform polyhedra has been established.

A similar approach is handled in this article, in which the Jitterbug-like set is first defined with respect to its group of symmetries. Then, an enumeration is carried out, resulting in the existence of two infinite classes in the dihedral groups, and 20 types in the tetra-, octa- and icosahedral groups of symmetry. Consequently, the geometrical properties are outlined, and peculiarities explained.

The article ends with an array of applications in architecture, engineering, art and mathematics, such as Fuller would have wanted it. Finally, since the Jitterbug-like transformer needs a new definition to complete the knowledge of its number and its full motion, a new name has been chosen here: dipolygonid.

1. INTRODUCTION

In various publications and lectures, Richard Buckminster Fuller introduced a geometrical structure which he called the "Jitterbug", a set of eight identical regular triangles connected to one another by the vertices [Fig. 1(a)].

The structure is able to perform a symmetrical ex- and impansion motion, illustrating a transformation between the octahedron and cuboctahedron. As Clinton observed in his paper on expanding rigid structures [1], each triangle is subject to a translation-rotation along its symmetry axis. When starting from the position in the octahedron, these axes are the four triangular symmetry axes of the octahedron. When describing cylinders about the triangles along the axes, each vertex common to two triangles moves along the intersecting curve of the two cylinders.

Both Clinton and Stuart [2] extend the Jitterbug transformation by starting this process at other Platonic solids and some Archimedean solids too, thus establishing a number of Jitterbug-like transformers. The question arises now: how can these transformers be geometrically defined resulting in a complete classification, and what is their number?

2. MATHEMATICAL APPROACH

In attempting to create a geometrical definition suitable for the Fuller-Stuart-Clinton transformations some preliminary observations appear:

1. Each transformation starts from a Platonic solid† or an Archimedean solid,‡ while certain rotational symmetries of that solid remain.§
2. The transformers are not symmetrical with respect to reflections which leave the solid invariant.
3. The structures are composed of one or two types of polygons, all having equal edge length.¶
4. The motion of the vertices is along the intersecting curve of two circumscribed cylinders.††

The previous observations make clear that the transformers have to be studied in connection with groups of rotations. Structures having a group of symmetries are usually best understood by extracting a fundamental part in accordance to a generating subset whose number of elements is minimal.‡‡

3. POLYGON-DIPOLYGON-DIPOLYGONID

3.1. Polygon

A polygon can also be defined by a rotation and a point, in an equivalent way to the definitions of Grünbaum [4] and Coxeter [5]. The advantage here is the consistency in definitions when generating higher groups of symmetries. Let A be a rotation and P a point. The image of the line segment $a = [P, A(P)]$ over $\text{gen}\{A\}$ (the cyclic group of rotations generated by A) is the regular polygon produced by A in P .

If $\#\text{gen}\{A\}$ is finite, say s , the polygon is composed of s vertices and s edges, all equal in length. If $\text{gen}\{A\}$ is discrete, the polygon is an infinite regular polygon.

For all points P outside of r_A , axis of A , the plane through P and perpendicular to r_A intersects r_A in M , whereas in the triangle $\Delta P, M, A(P)$ the angle $\sphericalangle P, M, A(P)$ is invariant and denoted by ψ , and will be referred to as the *central angle* of the rotation A .

Obviously $0 \leq \psi \leq \pi$.

Let A be distinct from the identity. Among the rotations of $\text{gen}\{A\}$, R and R^{-1} are those two whose central angle is the smallest besides the central angle 0 of the identity in the group. If $\text{gen}\{A\}$ is finite, the central angle of R and R^{-1} is $2\pi/s$. Then, clearly R and R^{-1} are generators of $\text{gen}\{A\}$. Let

$$A = R^d (1 \leq d < s) \rightarrow A = (R^{-1})^{s-d}.$$

Let the notations of R and R^{-1} be chosen such that

$$d \leq s - d \rightarrow d \leq \frac{s}{2}$$

d is called the *density* of the polygon, and $m = s/d$ the *polygonal value* of the rotation A . The notation for the polygon is $\{m\}$, and $m \geq 2$, for $d \leq s/2 \rightarrow 2 \leq s/d$.§§

†Clinton started a face-transformation from each of the five Platonic solids, although the octahedron provided the only coherent transformer: the Jitterbug. To be coherent, the remaining transformers had to be composed of coplanar pairs of polygons, as will be illustrated further. Even then, the tetrahedral transformer, composed of four coplanar pairs of triangles, would only be another appearance of the Jitterbug in one of its positions below the non-convex phase.

‡Stuart started a transformation from a semi-regular solid: the cuboctahedron. The transformation from cuboctahedron to rhombicuboctahedron is nicely shown on a flipmovie by the pages. However, the motion is restricted to the convex phase.

§Namely the rotations determined by those axes, along which the polygons transform. However, the transformers have all a symmetry group of rotations, e.g. Stuart's transformer of the cuboctahedron has the octahedral group of rotations (S_4) as its symmetry group, although the Jitterbug, which starts from the octahedron, has the tetrahedral group of rotations as its symmetry group (A_4), and not the octahedral. This can be understood by considering the octahedron as the semi-regular polyhedron of the tetrahedral group of isometries (S_4A_4), just like the cuboctahedron is in the octahedral group of symmetries ($S_4 \times I$).

¶Even in Clinton's edge transformations of the five Platonic solids the edges are merely digons.

††Or at least part of it, since the Fuller-Stuart-Clinton transformers are only determined as being convex, i.e. the motion ceases when the faces start intersecting each other.

‡‡To be compared to the Coxeter-Wythoff construction of the polyhedral kaleidoscope, which represents a set of three reflections as generating the group of isometries of a polyhedron. The kaleidoscope is associated with a fundamental region wherein the fundamental part of the polyhedron is conceived [3].

§§ $\{m\}$ is the Coxeter notation given to a regular polygon [5], while the polygonal value [6] implies a definition for density of a polygon, conform to Coxeter's approach [5].

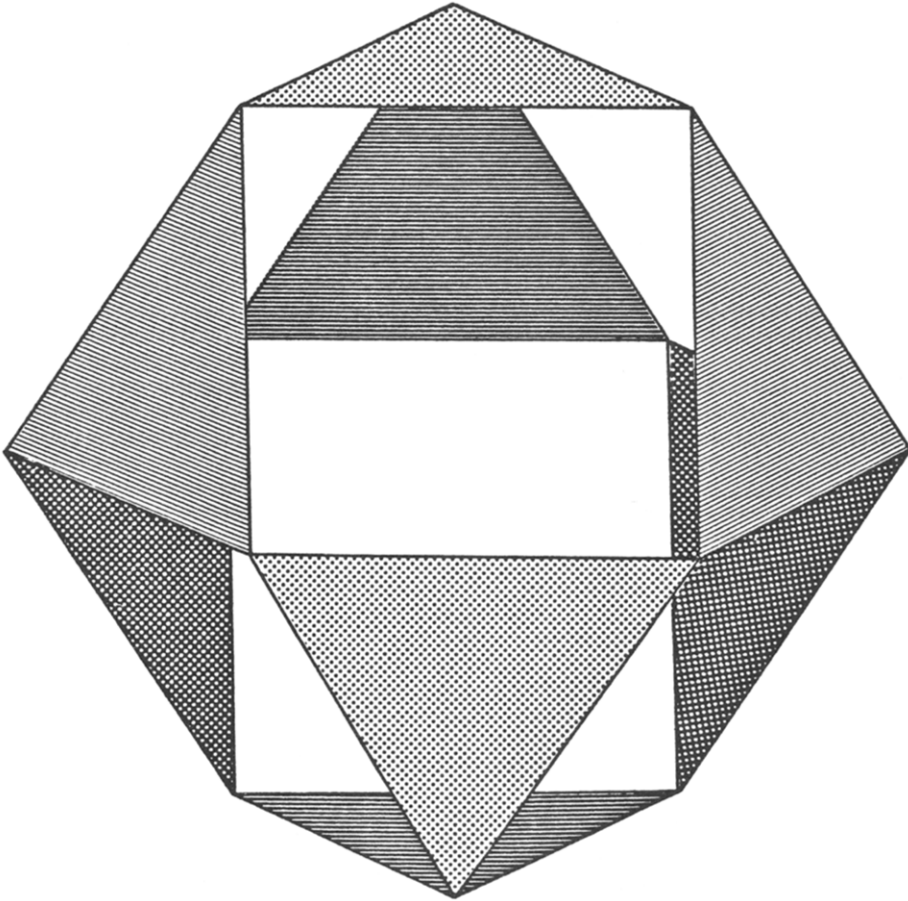


Fig. 1(a). The Jitterbug.

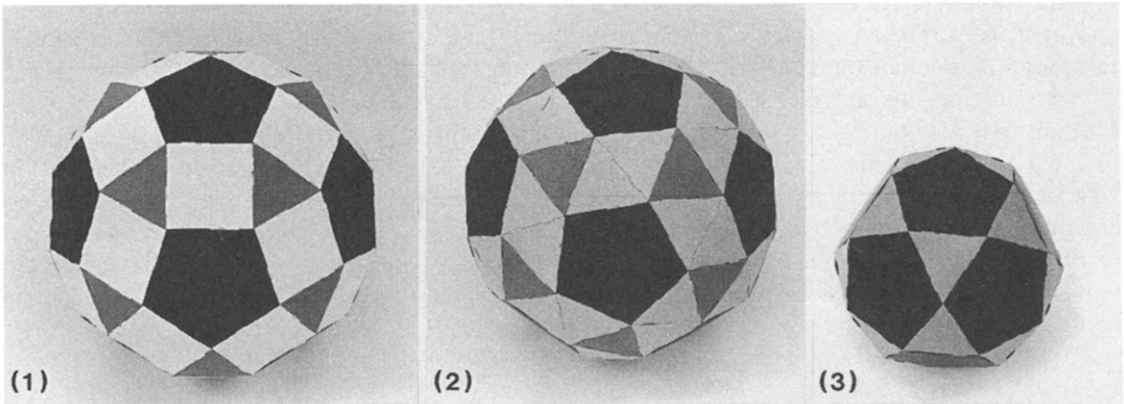


Fig. 1(b). Clinton's face-transformation can also be adapted to the icosidodecahedron. The transformation is illustrated in the (1) rhombicuboctahedron, (2) snub dodecahedron and (3) icosidodecahedron.

Hence, if m is a natural number > 2 , $\{m\}$ is the regular convex polygon composed of m edges and m vertices. If m is rational, $\{m\}$ is a regular star polygon of order s and density s/m .

Since $A = R^d$, the central angle of A can be calculated:

$$\psi_A = \frac{2\pi}{s} \cdot d = \frac{2\pi}{\frac{s}{d}} = \frac{2\pi}{m}.$$

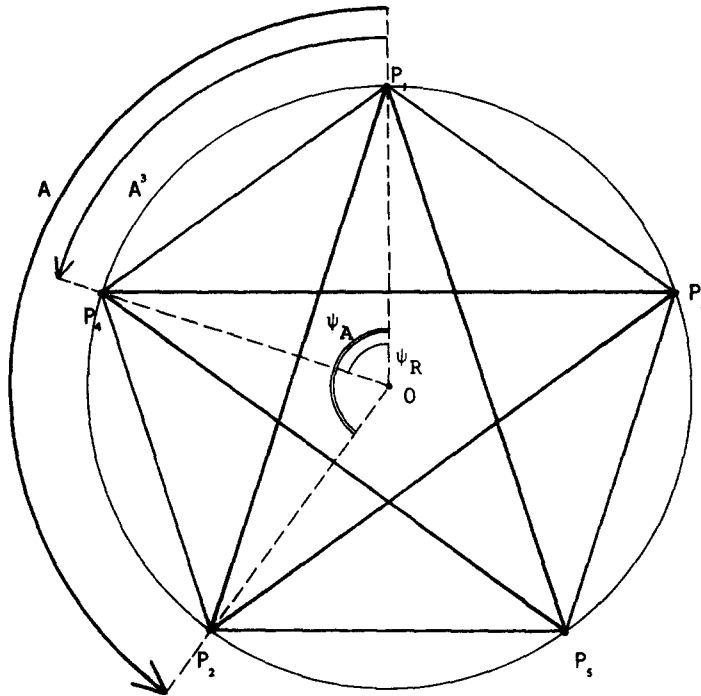


Fig. 2

Figure 2 illustrates an example where A has a central angle of $4\pi/5$, $\text{gen}\{A\} = \{E, A, A^2, A^3, A^4\}$ and $s = 5, d = 2$ and R is the rotation of a central angle $2\pi/5$.

If $s = 1$, the polygon $\{1\}$ is a monogon, i.e. composed of 1 vertex and an edge of length 0.†

If $s = 2$, the polygon $\{2\}$ is a digon, being composed of two collapsing edges and having two vertices P and $A(P)$. Although degenerate, the digon will be considered as a real polygon, and will appear to be of great importance further on. When $P \in r_A$, axis of A , the degenerate polygon is composed of s collapsing edges of length 0, and contains s coinciding vertices P .

From here on, the order of A will be supposed to be finite and > 1 . The polygonal value of a rotation indicates that any polygon produced in any point is of type $\{m\}$.

The whole process described here means no more than looking at a polygon from the point of view of rotational symmetry. Clearly A^{-1} produces an identical polygon $\{m\}$ in P . The definition determines a regular polygon as being a closed, broken line segment in a plane, perpendicular to r_A . The polygon indicates a maximal bounded subset of the plane, which will be called the polygonal face, or simply the face of the polygon. Polygonal faces will be used for constructing polyhedra [7].

3.2. Dipolygon

Each group of rotations has a point of invariancy O , being the one point of intersection of all axes of the rotations. Hence, the next step in the construction of a solid definition is to consider two rotations A and B whose axes intersect in one point O .

A produces $\{m\}$ in P , and B produces $\{n\}$ in P . This pair of polygons will be called a *dipolygon*, produced by the base $\{A, B\}$ in P (Fig. 3).

Consequently three more bases produce the same dipolygon in P : $\{A, B^{-1}\}, \{A^{-1}, B\}$ and $\{A^{-1}, B^{-1}\}$ (Fig. 4).

Dipolygonal specifications. A has order s , polygonal value m ; B has order t , polygonal value n .

The dipolygonal angle θ : r_A and r_B form in O the angles θ and $\pi - \theta$, where the choice for this

†When A is the identity, E .

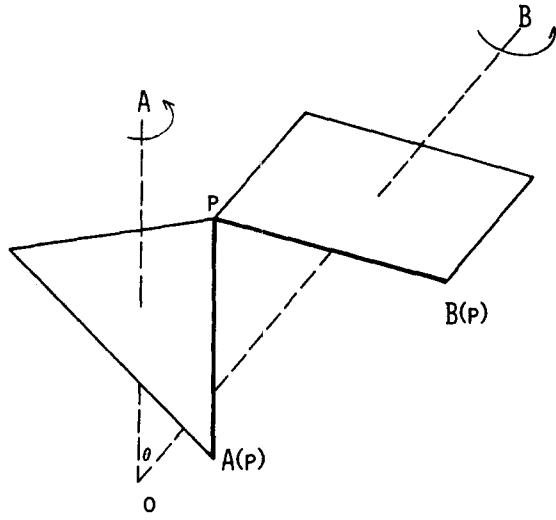


Fig. 3

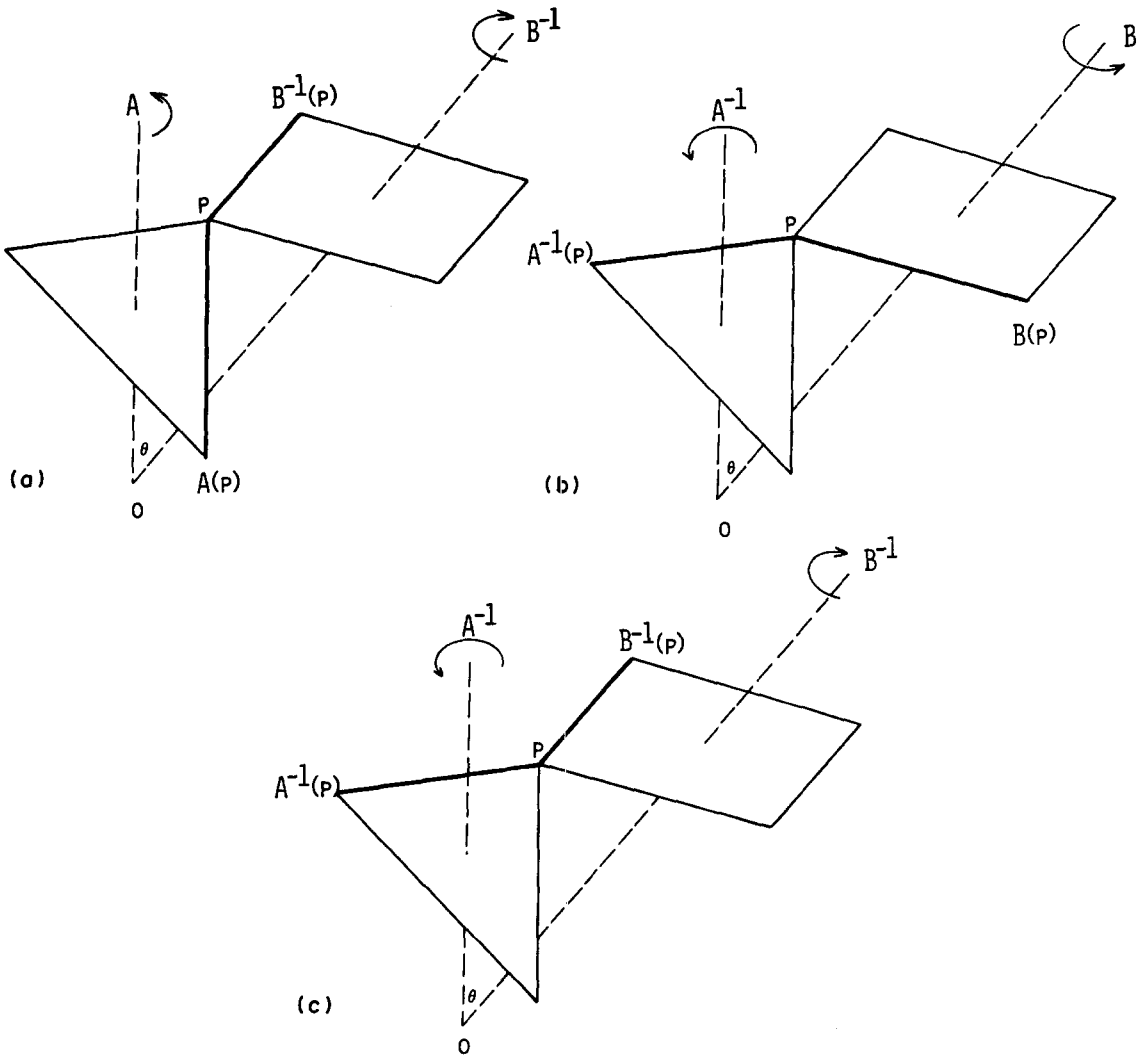


Fig. 4

notation is such that:

$$\theta \leq \pi - \theta \rightarrow 2\theta \leq \pi \rightarrow \theta \leq \frac{\pi}{2} \rightarrow 0 < \theta \leq \frac{\pi}{2} \leq \pi - \theta < \pi$$

- {m} has center M
- {n} has center N.

Also, the following properties exist: (a) the planes determined by the polygons {m} and {n}, are perpendicular to r_A and r_B resp., in the points M and N resp.; (b) the dihedral angle of these planes is θ (or the suppl. π - θ).

Now consider the circumscribed cylinders of {m} and {n}. These are simply defined by r_A and P, and r_B and P. When the radii of the cylinders have different length, the intersection will be composed of two distinct curves, which have central inverse symmetry in O [Fig. 5(a)]. P belongs to one of these curves. When the cylinders are equiradial (R_A = R_B), the two curves have two common points, altogether forming two intersecting ellipses that have a common smaller axis [Fig. 5(b)]. Still here, the intersection can be considered as being composed of two centrally inverse curves [Fig. 5(c)].

When P moves along the curve to which it belongs, even in the case of equiradial cylinders, in each position a dipolygon can be produced by the base {A, B}. Such a dipolygon is a transformed image of the first dipolygon, by a translation rotation of {m} along r_A, and of {n} along r_B. This transformation will be called the *uniform motion* of the dipolygon.

An equation for the intersection of the cylinders is calculated when a left-oriented base (X, Y, Z) is chosen as in Fig. 6. A and B are chosen such that for the radii R_A and R_B of the cylinders:

$$R_A \geq R_B; \quad \theta = \angle |\overline{OM}, \overline{ON}|; \quad \mu = \angle |\overline{X}^+, \overline{OP}_1|.$$

The equations of the cylinders are:

$$C_A \rightarrow x^2 + y^2 = R_A^2$$

$$C_B \rightarrow \cos^2 \theta \cdot x^2 + y^2 + \sin^2 \theta \cdot z^2 - 2 \sin \theta \cdot \cos \theta \cdot xz = R_B^2.$$

The parameter equation of C_A ∩ C_B is:

$$x = R_A \cos \mu$$

$$y = R_A \sin \mu$$

$$z = \frac{R_A \cos \theta \cdot \cos \mu \pm \sqrt{R_B^2 - R_A^2 \cdot \sin^2 \mu}}{\sin \theta},$$

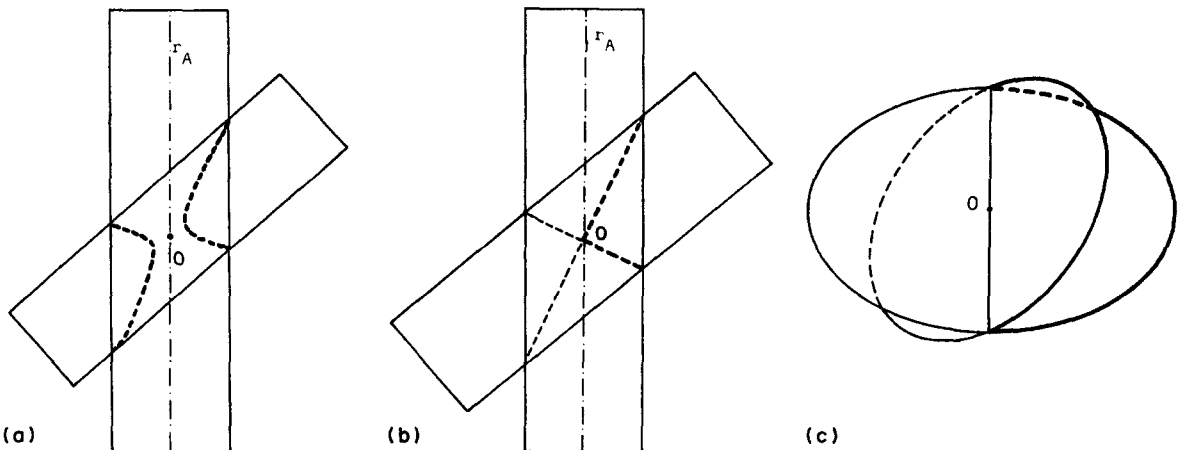


Fig. 5

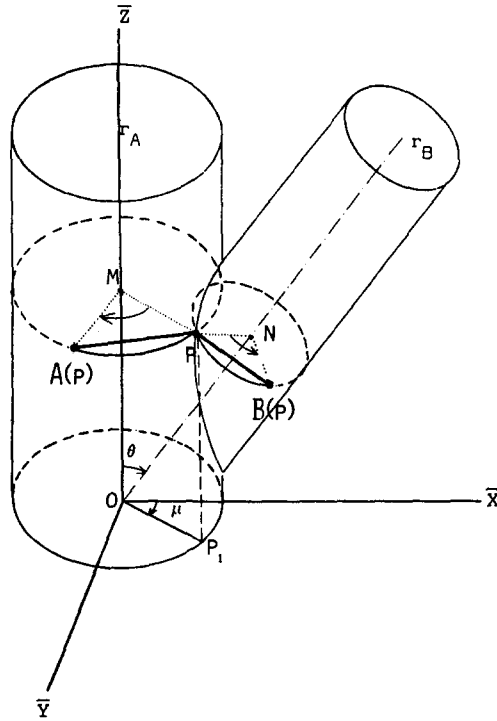


Fig. 6

where $|\sin \mu| \leq R_B/R_A$. Hence, the curve along which P moves is indicated by:

$$0 \leq |\mu| \leq \sin^{-1} \frac{R_B}{R_A} = \mu_c,$$

while the second curve of the intersection is given by

$$\mu + \pi.$$

The curve along which P moves will be referred to as the *path* of the uniform motion.

The sign (\pm) before the square root provides two values for z with each value for μ , except when $|\mu| = \mu_c$. The part of the curve determined by (+) is called the upper half of the path, and the (-) part the lower half.

The axes r_A and r_B determine a plane ω . If S denotes the reflection in ω , S leaves both cylinders and the path invariant. Some special positions with respect to ω will be observed.

(a) *Chiral positions.* The dipolygon produced by $\{A, B\}$ in $S(P)$ is the reflected image of the one in P . These dipolygons are enantiomorphous positions of each other (dextro and laevo). Since A and A^{-1} , B and B^{-1} are transformed operations by $S(A^{-1} = SAS, B^{-1} = SBS)$, all the properties of a dipolygon with respect to its base hold for the laevo position, provided the base is inverted, i.e. the rotations are inverted.

(b) *Extreme positions.* if $P \in \omega, S(P) = P$. Such a position is self-enantiomorphous and ω is a symmetry plane of this position of the dipolygon. There are two such positions on the path, called the extreme positions. The plane ω is perpendicular to $\{m\}$ and $\{n\}$, while $M, N, P, O \in \omega$.

In an extreme position $\mu = 0$, and the coordinates of P become:

$$(R_A, 0, R_A \cot \theta \pm R_B \operatorname{cosec} \theta).$$

The extreme position in the upper half is called the maximum position. Here

$$\Delta M, P_{\max}, N = \pi - \theta \text{ (right or obtuse).}$$

The extreme position in the lower half is called the minimum position. Here

$$\Delta M, P_{\min}, N = \theta \text{ (right or sharp).}$$

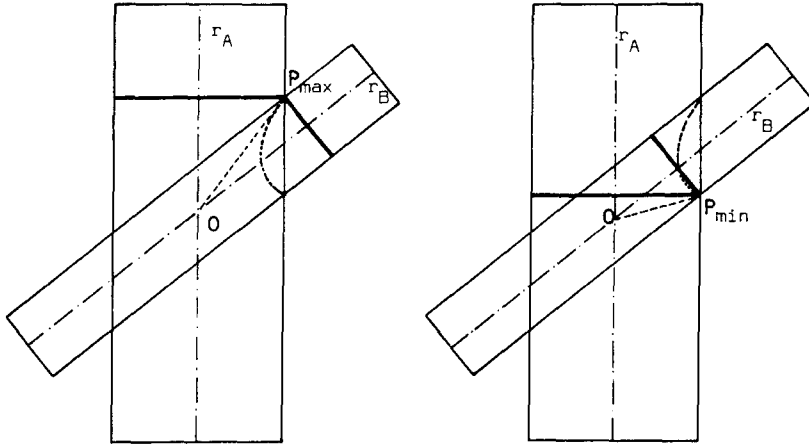


Fig. 7

However, if $\theta = \pi/2$, the plane γ through r_B and perpendicular to ω is a symmetry plane for the two cylinders and hence for the path. Then, each of the extreme positions may represent the maximum or minimum position.

From the equations follows: when the dipolygon moves along the path between two extreme positions, $\{n\}$ describes a rotation over π . Halfway, when $\{n\}$ has rotated over $\pi/2$, the rotation of $\{m\}$ has reached its maximal angle

$$|\mu| = \mu_c.$$

The chiral positions in μ_c and $-\mu_c$ are called the central positions of the dipolygon.

From the equations also follows:

(a) The translation of $\{m\}$ happens between the extreme positions, where the sense reverses; the translation of $\{n\}$ happens between the extreme positions and the central positions. In each of these positions, the sense reverses.

(b) The rotation of $\{m\}$ happens between central positions, where the sense reverses; the rotation of $\{n\}$ is in one sense all along the path.

Hence, while passing a central position $\{m\}$ keeps its sense of translation, but reverses its sense of rotation, while $\{n\}$ reverses its sense of translation, but keeps its sense of rotation.

When $R_A = R_B$, $\mu_c = \pi/2$. Then, in a central position M coincides with O and since PN and r_B are perpendicular, also N coincides with M and O . The points of the path, in which the dipolygon is in a central position are the intersecting points of the upper and lower-half ellipses on their common smaller axis. If also the dipolygon is regular, i.e. being composed of two congruent polygons, two more planes of special interest can be observed: α and β , bisector planes of r_A and r_B , chosen such that:

$$P_{\max} \in \alpha, \quad P_{\min} \in \beta.$$

Thus, α is a symmetry plane for the dipolygon in the upper half-ellipse, while β is for the lower half-ellipse.

3.3. Dipolygonid

If G denotes the group of rotations generated by A and B , all the axes of the rotations of G intersect in O , point of invariancy of G . G may be discrete or finite.

The image of the dipolygon over G is called the *dipolygonid*, produced by the base $\{A, B\}$ in P (Fig. 8).

By this construction the dipolygonid is invariant over G . Clearly the dipolygonid is also produced by the other three bases:

$$\{A^{-1}, B\}, \{A, B^{-1}\}, \{A^{-1}, B^{-1}\}.$$

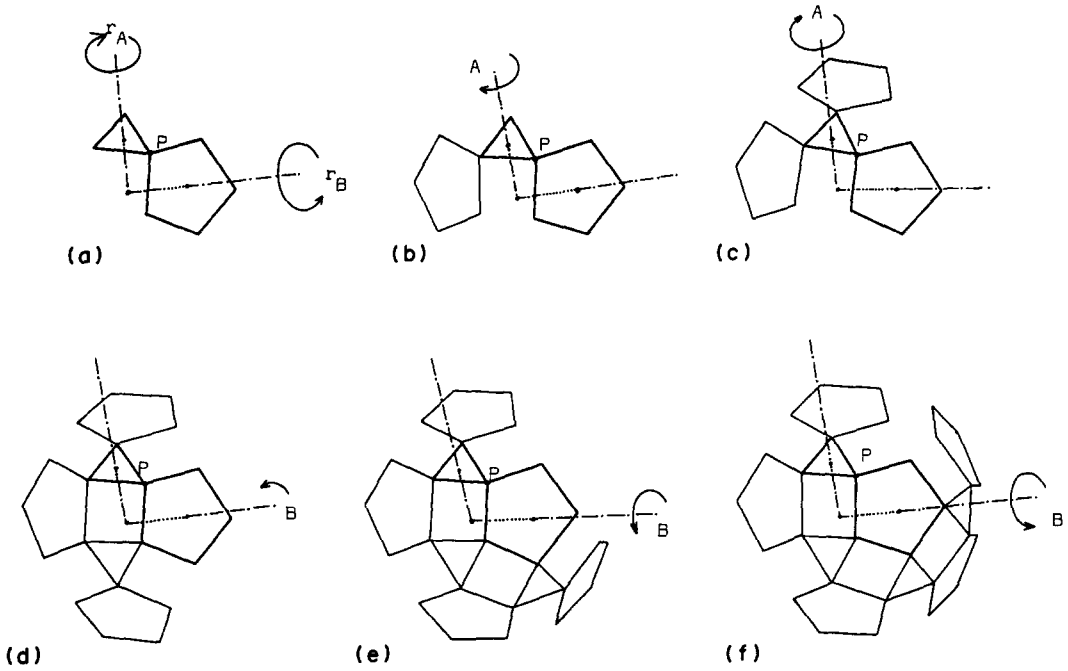


Fig. 8

Moreover, it can be produced in any vertex $R(P)$, where $R \in G$. The base $\{A, B\}$ is then transformed by R into a set $\{RAR^{-1}, RBR^{-1}\}$ which act like a base for the transformed dipolygon in $R(P)$.

Since $\{RAR^{-1}, RBR^{-1}\}$ clearly is a generating set of G too, the dipolygonid is also produced in $R(P)$ by the base $\{RAR^{-1}, RBR^{-1}\}$.

The smallest subset of the dipolygon in P whose image over G is the dipolygonid is the couple of edges a and b (Fig. 10). This two-edge is the fundamental part of the dipolygonid with respect to G .

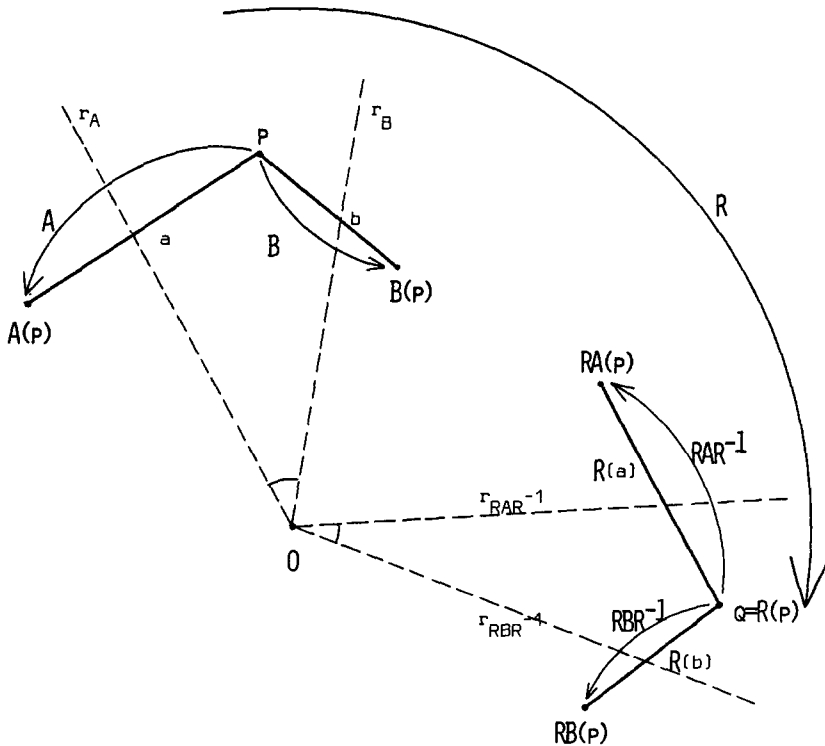


Fig. 9

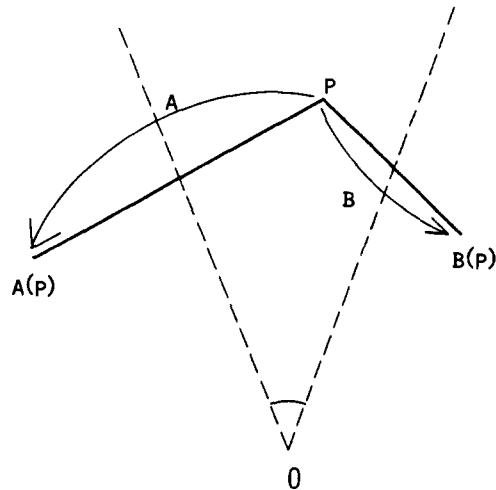


Fig. 10

Each position of the dipolygon produced by $\{A, B\}$ in P has its image over G , thus creating a dipolygonid. When the dipolygon describes its uniform motion along the path, all the transformed dipolygons in $R(P)$ do simultaneously. This motion is called the uniform motion of the dipolygonid (Fig. 11).

4. JITTERBUG AND DIPOLYGONIDS

It can easily be seen that this definition for a dipolygonid is appropriate to the Fuller–Stuart–Clinton transformers, holding the following generalizations:

- Since G may be discrete, so will the dipolygonid be composed of an infinite number of polygons, yet able to perform the transformations.†
- The dipolygonid has not necessarily one edge length. Depending on the position of P , the dipolygonid may have two different edge lengths.
- Along the path of uniform motion the dipolygonid becomes non-convex. In fact the uniform motion rather resembles a pulsating motion from maximum position over central-1, minimum, central-2 to maximum position.

5. FINITE DIPOLYGONIDS

Our next concern is the search for dipolygonids which are composed of a finite number of polygons and vertices. This will be the case if G is finite. Then, the question is brought back to the investigation of the finite groups of rotations, which are well established [5].

If G is finite, the order will be denoted by g . Then, the dipolygonid is composed of g vertices theoretically, and hence, of g dipolygons.

G will be finite, only if A and B belong to one of the finite groups of rotations and generate a subgroup at least. This will solely depend of the orders of A and B , and the angle θ formed by their axes in O . Since r_A and r_B are distinct, however, the cyclic groups can be excluded.

Table 1 classifies the remaining finite groups of rotations by their number of elements and the conjugate maximal cyclic subgroups. The latter numbers indicate the types of axes in Table 2.

In Table 3, a summary is given of all the possible angles between axes of a group. An axis is represented by the order of the maximal cyclic subgroup of rotations, having this axis.

†The major part of Clinton's paper deals with transformations (face, edge and vertex) of flat tessellations. Those are composed of an infinite number of polygons. Such a transformer can be considered as a dipolygonid whose base $\{A, B\}$ has its axes intersecting at infinity. Then, $R_A//R_B$ and the dipolygonid will be planar, and G discrete.

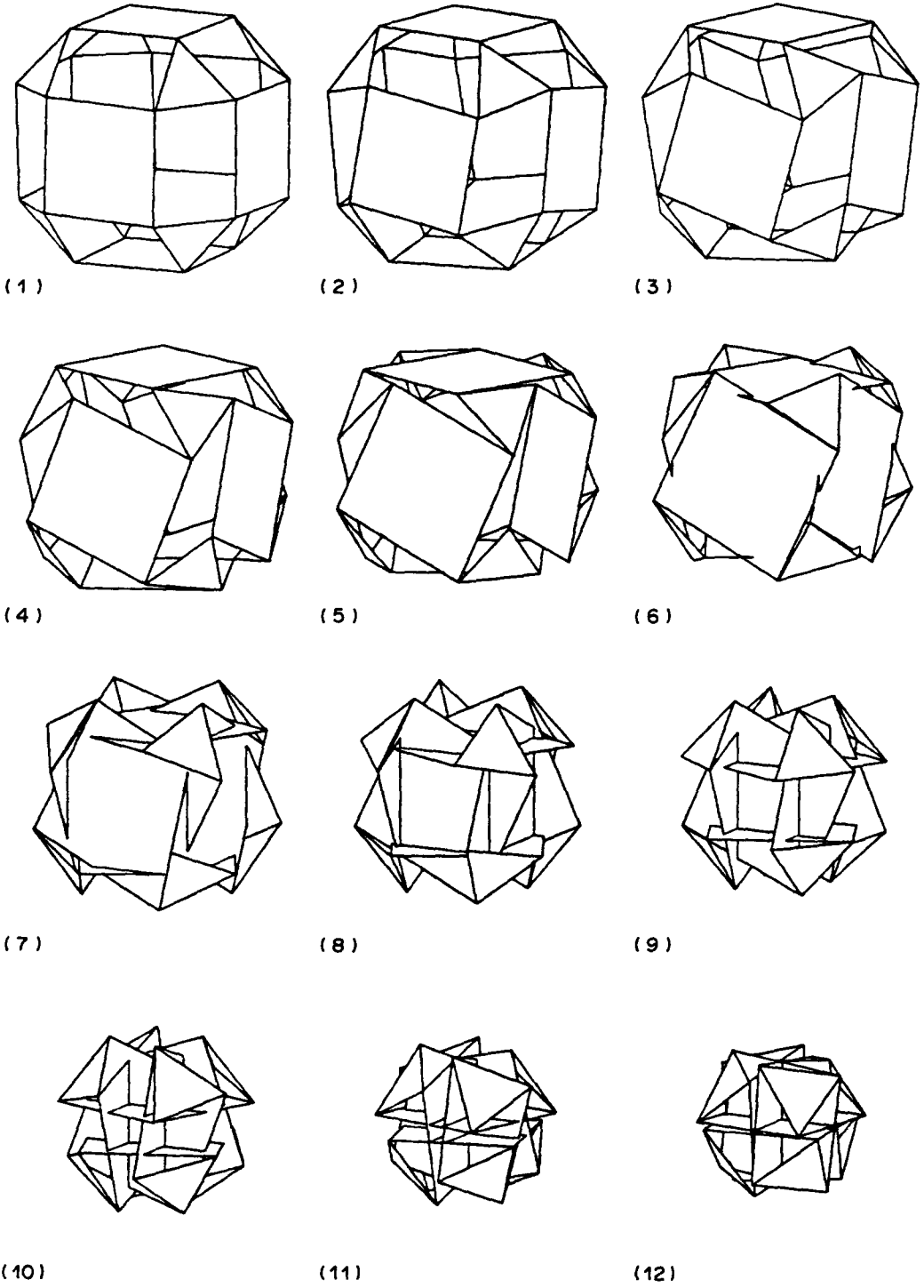
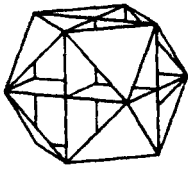
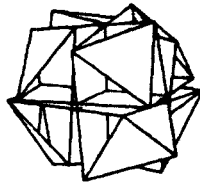


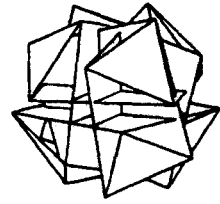
Fig. 11 (1-12)



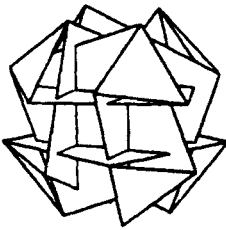
(13)



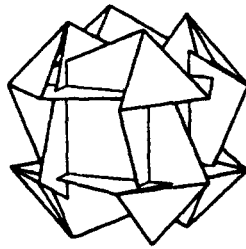
(14)



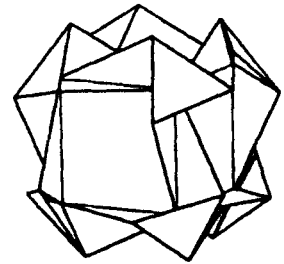
(15)



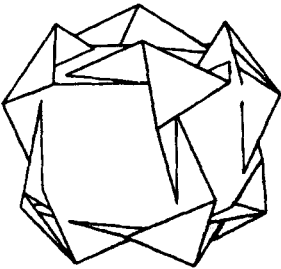
(16)



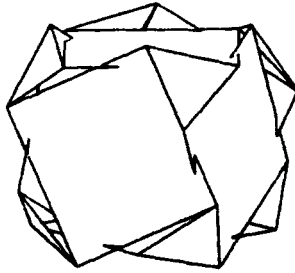
(17)



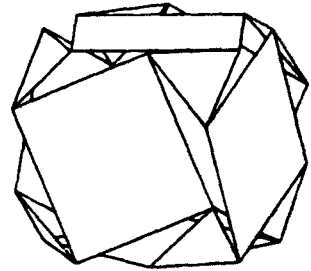
(18)



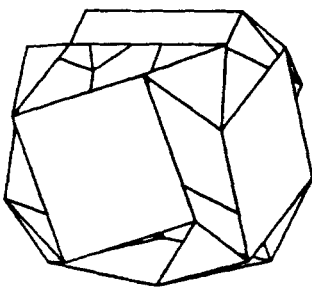
(19)



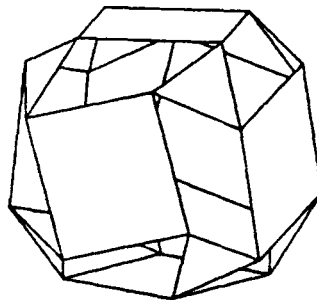
(20)



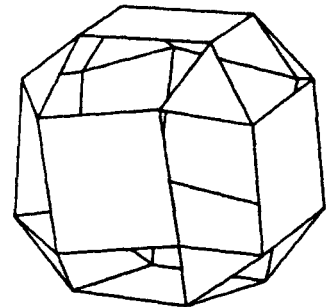
(21)



(22)



(23)



(24)

Fig. 11 (13-24)

Table 1

GROUP	ORDER	CONJUGATE CYCLIC SUBGROUPS	
		number	order
Dihedral	2n	n	2
		1	n
Tetrahedral	12	3	2
		4	3
Octahedral	24	6	2
		4	3
		3	4
Icosahedral	60	15	2
		10	3
		6	5

Table 2

GROUP	NUMBER OF AXES
Dihedral (D_n)	$n + 1$
Tetrahedral	7
Octahedral	13
Icosahedral	31

Out of Table 3 a summary can be realized of all possible pairs of rotations in the dihedral, tetra-, octa- and icosahedral groups with respect to the order of these rotations and the angle of their axes. Table 4 shows this summary, together with the groups that are generated by these pairs.

In C_5 , the cyclic group of rotations of order 5, four elements occur of order 5, namely the rotations of polygonal value 5 and $5/2$.†

All other pairs of rotations besides those mentioned in Table 4 result as generators of discrete groups of rotations. Apart of the two classes of pairs generating the dihedral groups, there are two types of pairs in the tetrahedral, four in the octahedral, and 14 in the icosahedral group of rotations.

Hence, there is a corresponding amount of dipolygonid types, when the pairs of generators represent a base. If g represents the order of G , s of A , and t of B , the number of the dipolygonid's elements is: vertices— g ; polygons $\{m\}$ — g/s ; polygons $\{n\}$ — g/t ; edges— $2g$.

The following notation will be used for a finite dipolygonid:

$$\frac{g}{s} \{m\} + \frac{g}{t} \{n\} | \theta \ddagger$$

6. CLASSIFICATION OF THE FINITE DIPOLYGONIDS

6.1. Dihedral (D_n)

Two infinite classes are associated to each of the infinite classes of bases:

$$(A) \quad n\{2\} + n\{2\} | \frac{k}{n} \cdot 180^\circ$$

where $n = 2$ and $k = 1$, or $n > 2$ and $0 < k < n/2$ (and k and n are coprime). These dipolygonids have the shape of non-planar polygonal zigzag lines. If both sets of digons have equal length, they represent "Petrie-polygons" [3, 5].

$$(B) \quad n\{2\} + 2\left\{\frac{n}{k}\right\} | 90^\circ.$$

These dipolygonids have the shape of rectangular $\{n/k\}$ -prisms in extreme positions.

†Namely the rotations over $\pm 2\pi/5$ (polygonal value 5) and over $\pm 4\pi/5$ (polygonal value $\frac{5}{2}$).

‡In accordance to the notation of a uniform polyhedron by indicating the numbers of different types of polygons as a summation [8].

Table 3

GROUP	SYMBOL	AXES	ANGLE (SUPPLEMENT)
DIHEDRAL ($n=2,3,\dots$)	D_n	$2 \sim 2$	$\frac{k}{n} \cdot 180^\circ$, $k \in \mathbb{N}$, $0 < k \leq \frac{n}{2}$
		$2 \sim n$	90° (90°)
TETRAHEDRAL	A_4	$2 \sim 2$	90° (90°)
		$2 \sim 3$	$54^\circ 44' 08''$ (125°15'52")
		$3 \sim 3$	$70^\circ 31' 44''$ (109°28'16")
OCTAHEDRAL	S_6	$2 \sim 2$	60° (120°) 90° (90°)
		$2 \sim 3$	$35^\circ 15' 52''$ (144°44'08") 90° (90°)
		$2 \sim 4$	45° (135°) 90° (90°)
		$3 \sim 3$	$70^\circ 31' 44''$ (109°28'16")
		$3 \sim 4$	$54^\circ 44' 08''$ (125°15'52")
		$4 \sim 4$	90° (90°)
		ICOSAHEDRAL	A_5
$2 \sim 3$	$20^\circ 54' 19''$ (159°05'41") $54^\circ 44' 08''$ (125°15'52") $69^\circ 05' 42''$ (110°54'18") 90° (90°)		
$2 \sim 5$	$31^\circ 43' 03''$ (148°16'57") $58^\circ 16' 57''$ (121°43'03") 90° (90°)		
$3 \sim 3$	$41^\circ 48' 37''$ (138°11'23") $70^\circ 31' 44''$ (109°28'16")		
$3 \sim 5$	$37^\circ 22' 39''$ (142°37'21") $79^\circ 11' 16''$ (100°48'44")		
$5 \sim 5$	$63^\circ 26' 06''$ (116°33'54")		

Table 4

A ~ B	θ	gen{A, B}
2 ~ 2	$\frac{k}{n} \cdot 180^\circ \dagger$	D_n
2 ~ 3	20°54'19"	A_5
	35°15'52"	S_4
	54°44'08"	A_4
	69°05'42"	A_5
2 ~ 4	45°	S_4
2 ~ 5	31°43'03"	A_5
	58°16'57"	A_5
2 ~ n	90°	D_n
3 ~ 3	41°48'37"	A_5
	70°31'44"	A_4
3 ~ 4	54°44'08"	S_4
3 ~ 5	37°22'39"	A_5
	79°11'16"	A_5
4 ~ 4	90°	S_4
5 ~ 5	63°26'06"	A_5

† $n \geq 2$: if $n = 2, k = 1$; if $n \geq 3, 1 \leq k < n/2, k$ and n coprime.

The example $3\{2\} + 2\{3\} | 90^\circ$ in D_3 is illustrated in Fig. 12.

6.2. Tetrahedral

See Fig. 13; T_1-T_2 .

6.3. Octahedral

See Fig. 14; O_1-O_4 .

6.4. Icosahedral

See Fig. 15; I_1-I_{14} .

Since the number of polygons $\{m\}$ is g/s , as is also the index of the cyclic subgroup of order s in G (the number of s -fold axes in G), clearly the number of polygons along one axis is known.

For example, in I_3 , 12 pentagons occur along 6 five-fold axes. Hence, two pentagons have a common axis. The question rises: do these polygons occur on the same side or different sides of O ?

The answer is easily found by observing the two-fold rotation whose axis is perpendicular to ω . If this rotation is in G , it maps the dipolygon within the dipolygonid on the opposite side of both axes of the dipolygon's base. (See Diagram 1.)

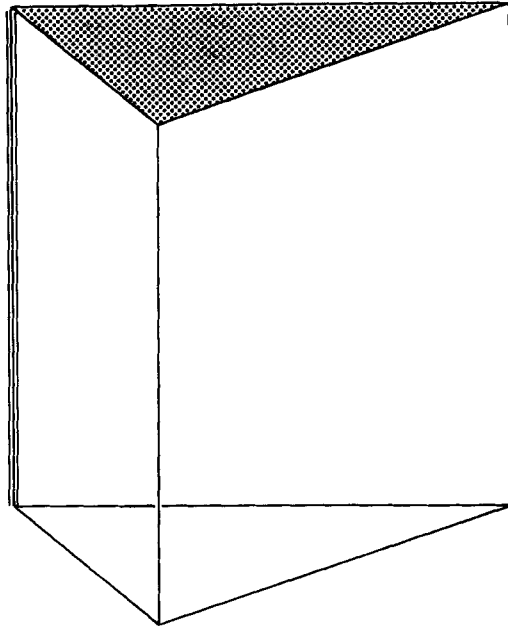
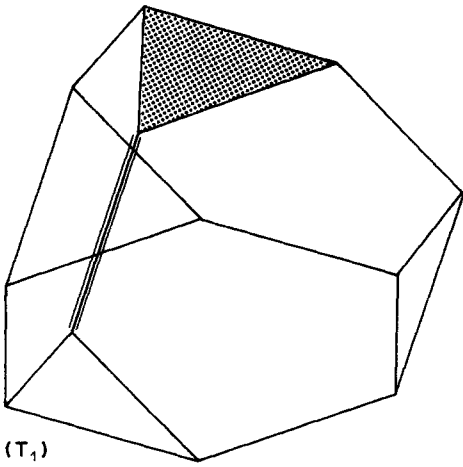
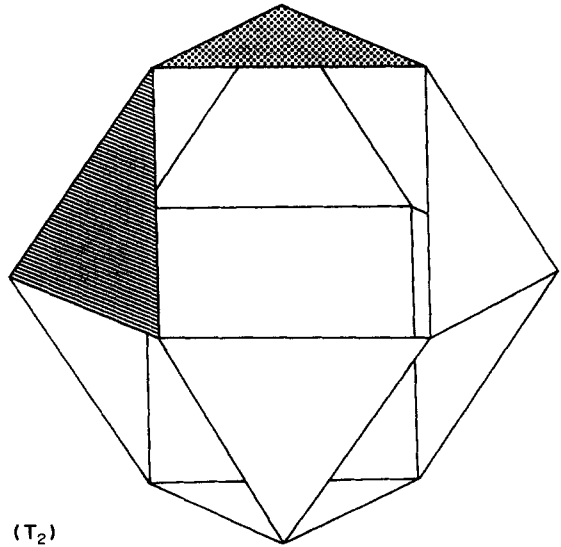


Fig. 12



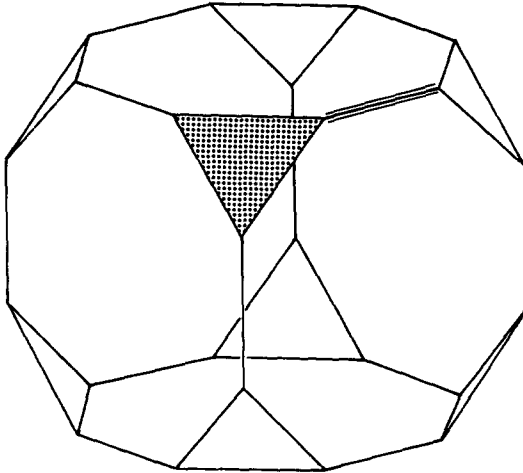
(T₁)

Fig. 13(a). $T_1 \rightarrow 6\{2\} + 4\{3\} | 54^\circ 44' 08''$.



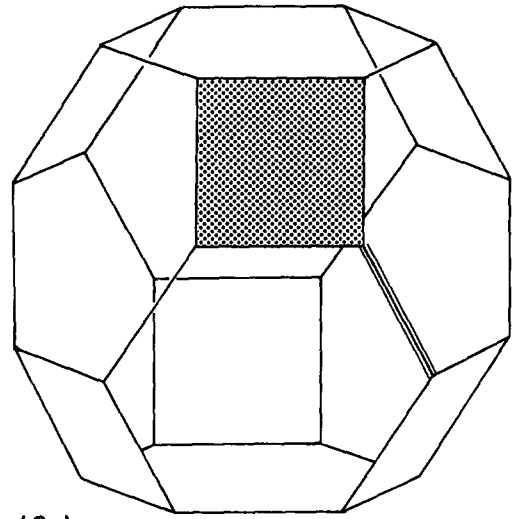
(T₂)

Fig. 13(b). $T_2 \rightarrow 4\{3\} + 4\{3\} | 70^\circ 31' 44''$.



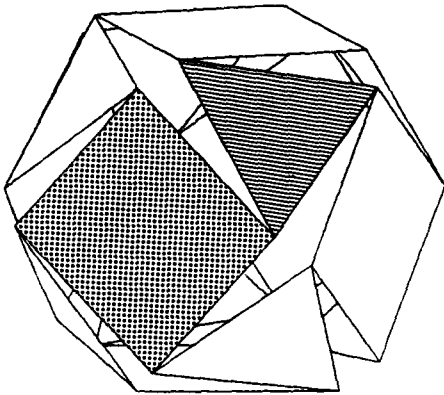
(O_1)

Fig. 14(a). $O_1 \rightarrow 12\{2\} + 8\{3\} | 35^\circ 15' 52''$.



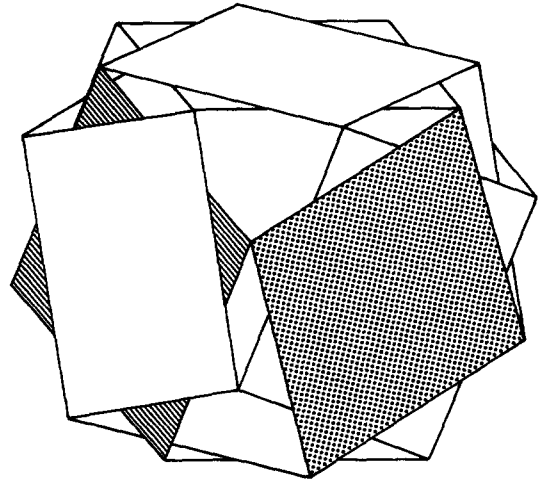
(O_2)

Fig. 14(b). $O_2 \rightarrow 12\{2\} + 6\{4\} | 45^\circ$.



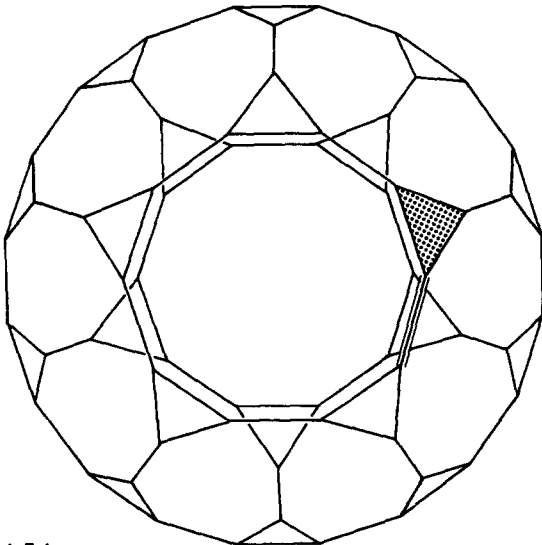
(O_3)

Fig. 14(c). $O_3 \rightarrow 8\{3\} + 6\{4\} | 54^\circ 44' 08''$.



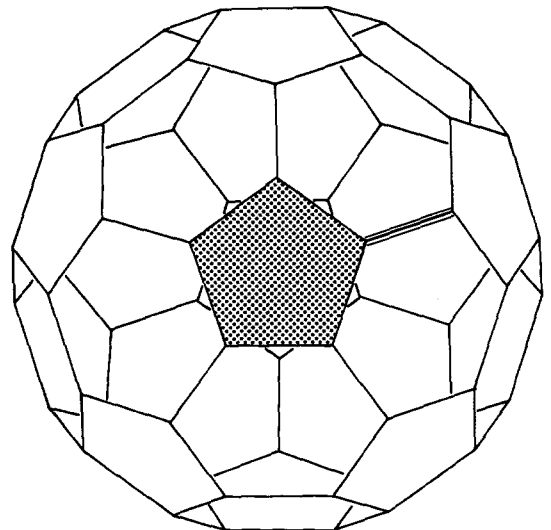
(O_4)

Fig. 14(d). $O_4 \rightarrow 6\{4\} + 6\{4\} | 90^\circ$.



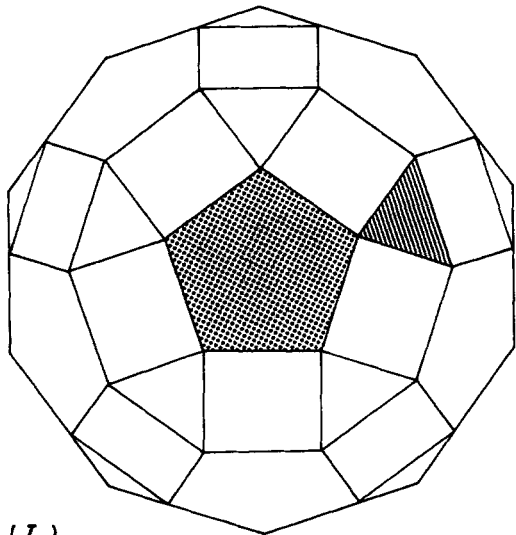
(I_1)

Fig. 15(a). $I_1 \rightarrow 30\{2\} + 20\{3\} | 20^\circ 54' 19''$.



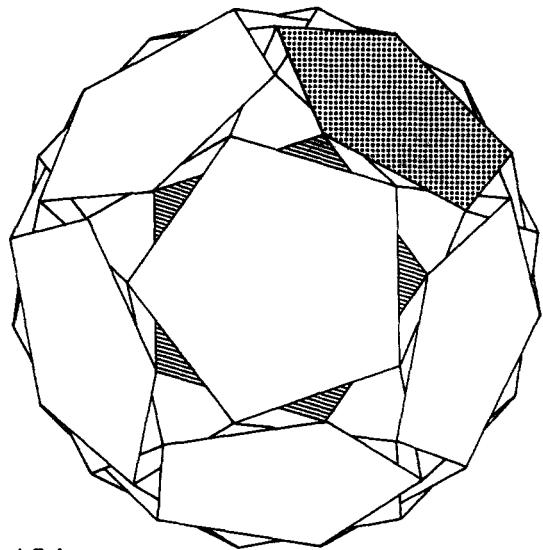
(I_2)

Fig. 15(b). $I_2 \rightarrow 30\{2\} + 12\{5\} | 31^\circ 43' 03''$.



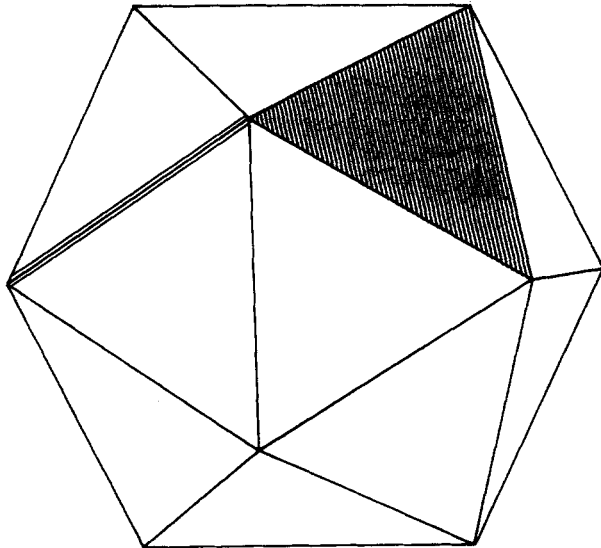
(I_3)

Fig. 15(c). $I_3 \rightarrow 20\{3\} + 12\{5\} | 37^\circ 22' 39''$.



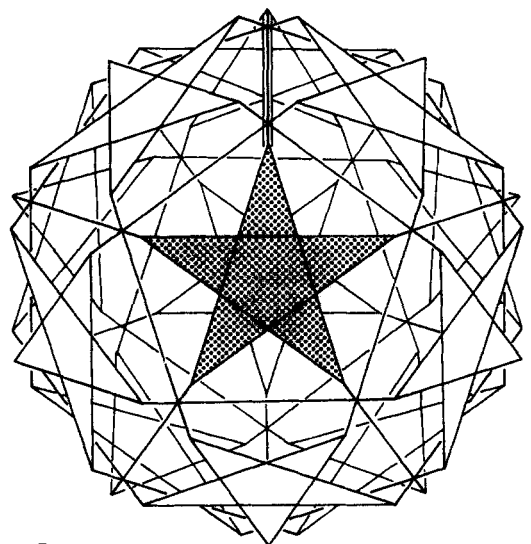
(I_4)

Fig. 15(d). $I_4 \rightarrow 12\{5\} + 12\{5\} | 63^\circ 26' 06''$.



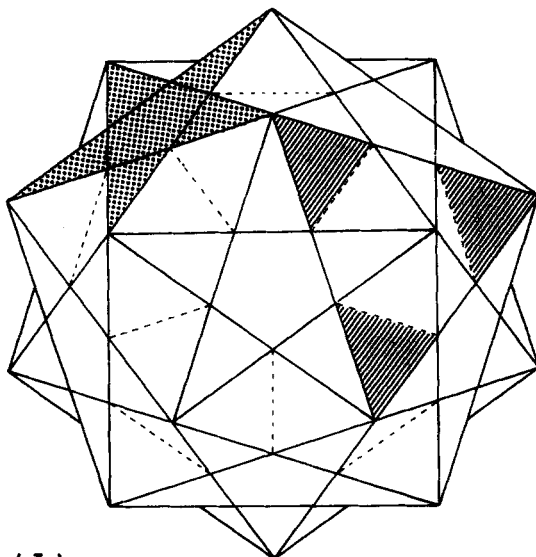
(I_5)

Fig. 15(e). $I_5 \rightarrow 30\{2\} + 20\{3\} | 69^\circ 05' 42''$.



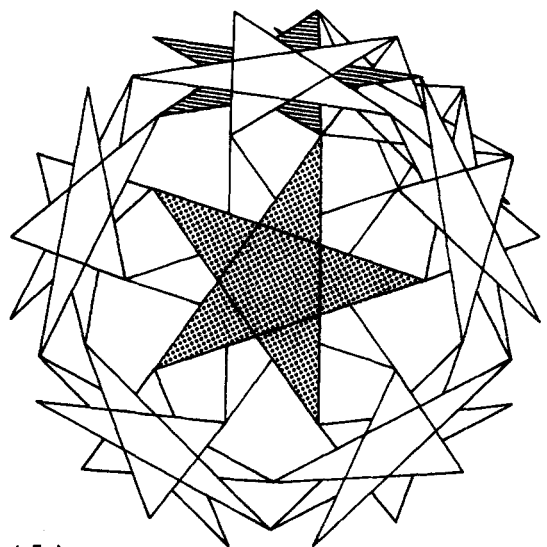
(I_6)

Fig. 15(f). $I_6 \rightarrow 30\{2\} + 12\{5/2\} | 58^\circ 16' 57''$.



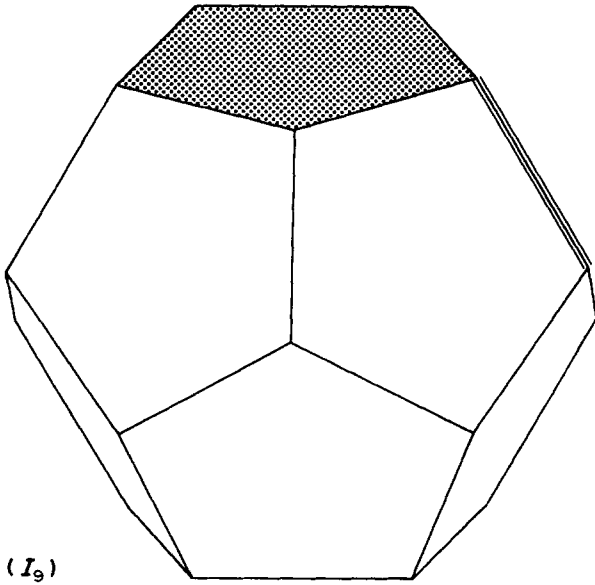
(I_7)

Fig. 15(g). $I_7 \rightarrow 20\{3\} + 12\{5/2\} | 79^\circ 11' 16''$.



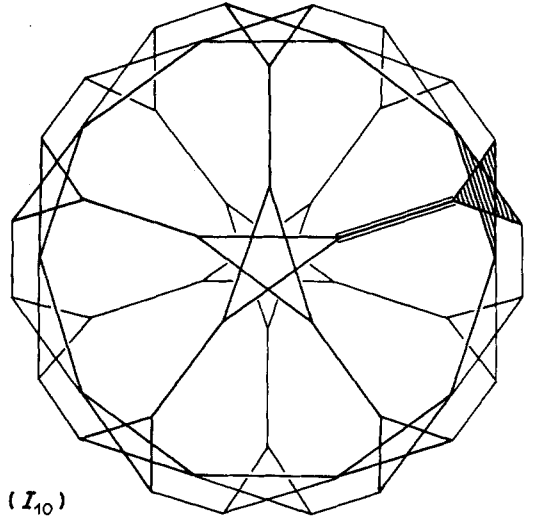
(I_8)

Fig. 15(h). $I_8 \rightarrow 12\{5/2\} + 12\{5/2\} | 63^\circ 26' 06''$.



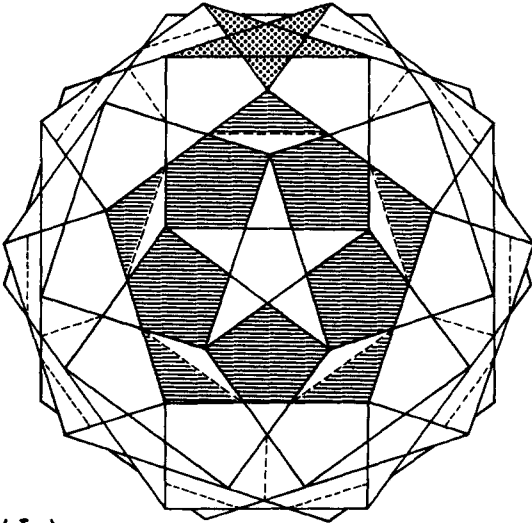
(I_9)

Fig. 15(i). $I_9 \rightarrow 30\{2\} + 12\{5\} | 58^\circ 16' 57''$.



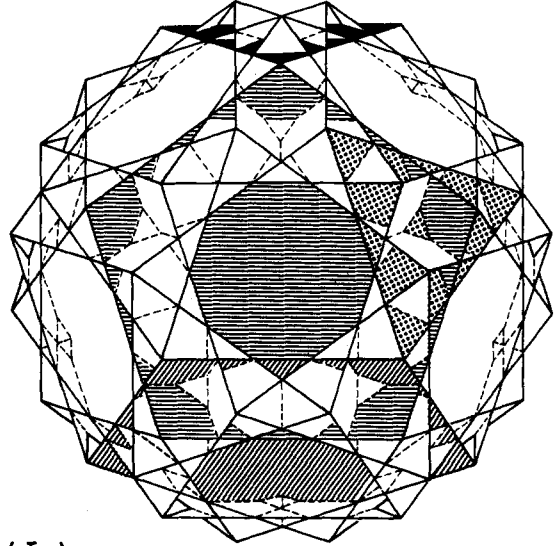
(I_{10})

Fig. 15(j). $I_{10} \rightarrow 30\{2\} + 12\{5/2\} | 31^\circ 43' 03''$.



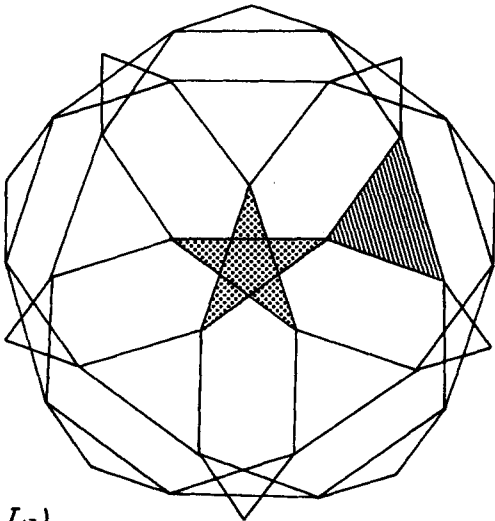
(I_{11})

Fig. 15(k). $I_{11} \rightarrow 12\{5\} + 12\{5/2\} | 63^\circ 26' 06''$.



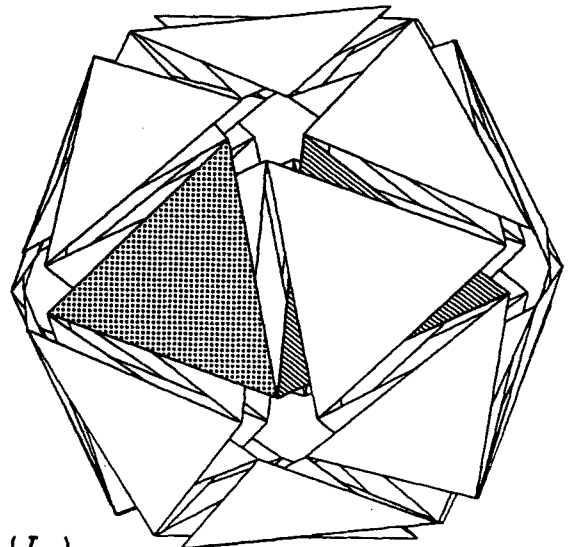
(I_{12})

Fig. 15(l). $I_{12} \rightarrow 20\{3\} + 12\{5\} | 79^\circ 11' 16''$. (In this illustration two different dipolygons have been shaded.)



(I_{13})

Fig. 15(m). $I_{13} \rightarrow 20\{3\} + 12\{5/2\} | 37^\circ 22' 39''$.



(I_{14})

Fig. 15(n). $I_{14} \rightarrow 20\{3\} + 20\{3\} | 41^\circ 48' 37''$.

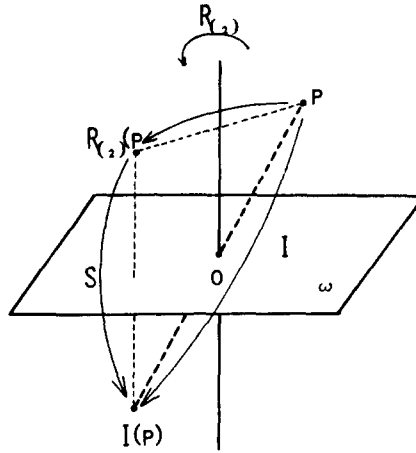


Diagram 1. The half-turn R is about an axis perpendicular to ω . Then $I = SR = RS$.

From Table 1 is found that the only exceptions for the two-fold rotation being in G are for the bases of type:

1. In D_n : $2 \sim 2 \mid \frac{k}{n} \cdot 180^\circ$ ($0 < k < \frac{n}{2}$, n odd, k and n coprime)
2. In A_4 : $3 \sim 3 \mid 70^\circ 31' 44''$

which correspond to the dipolygonids of class A in the odd dihedral groups D_n , and the dipolygonid T_2 .

In the first case, the polygons of type $\{m\}$ and $\{n\}$, sharing a common axis of order 2 are two digons of different edge length (although they may be equal too).

In the second case, two triangles of different edge length (or equal) share a common three-fold axis.

7. ASPECTS OF UNIFORM MOTION

Together with the dipolygon in P , and all the dipolygons in the points $R(P)$, where $R \in \text{gen}\{A, B\}$, the dipolygonid describes its uniform motion. Special positions of the dipolygon have their equivalent special positions of the dipolygonid.

7.1. Chiral positions

Each step in the production of a dipolygonid in $S(P)$ by the laevo base $\{A^{-1}, B^{-1}\}$ is the reflected operation under S of a step in the production of the dipolygonid in P by $\{A, B\}$. However, the dipolygonid in $S(P)$ is also produced by $\{A, B\}$. The set of both dipolygonids is also the image over G of the chiral dipolygons in P and $S(P)$, which are reflected images by S . Then, the set of dipolygonids is invariant over $G_S = \text{gen}\{A, B, S\}$, an extended group of G [9].

The dipolygonids are reflected images of each other under any reflection of G_S , and therefore can be called enantiomorphous (dextro and laevo) too.

7.2. Extreme positions

Maximum and minimum positions of the dipolygonid correspond with those of the dipolygon.

7.3. Central positions

A central position of the dipolygonid is produced when the dipolygon is in a central position. Figure 16 illustrates O_4 from the maximum to central position in steps.

Besides the two exceptions mentioned in Section 6, all the finite dipolygonids are composed of opposite polygons $\{m\}$ and $\{m\}'$ along the s -fold axes, and $\{n\}$ and $\{n\}'$ along the t -fold axes of $G = \text{gen}\{A, B\}$.

Since the centers of the polygons, M and M' , and N and N' each remain on equal distances of O during the uniform motion of the dipolygonid, the property holds for each position. During the uniform motion M or N may coincide with O .

Since $\{n\}$ reverses its sense of translation in a central position, N would only coincide with O when $R_A = R_B$ in both central positions. However, the sense of the translation of $\{m\}$ reverses in the extreme positions and hence, M may coincide with O , depending on R_A and R_B , or analogue, depending on the edge lengths of $\{m\}$ and $\{n\}$.

When $R_A = R_B$, M and N of the dipolygon coincide with O , and hence, so will all of the polygons have their center coinciding with O .

Before going into more details of equiradial dipolygonids, some more understanding of the symmetries in extended groups of isometries is needed.

8. EXTENDED GROUPS OF ISOMETRIES

Besides the finite groups of rotations, the remaining groups of isometries are distinguished by their containing of the central inversion in O (denoted by I) or not [5].

(a) *Groups containing I .* These groups all are the direct product of a finite group of rotations and the group $\{E, I\}$, which in Table 5 is denoted by the abbreviated symbol I .

(b) *Groups that do not contain I .* These groups are called "mixed groups". If G' is a group of rotations of order $2n$, containing a subgroup G of order n , the mixed group is $G \cup (G' - G)I$, which in Table 5 is denoted by $G'G$.

Each of these groups has an even order $2g$, and contains a subgroup of rotations of order g . The number of rotatory inversions (products of a rotation of G and I) is also g . A rotatory inversion is either a rotatory reflection (a product of a rotation and a reflection) or a reflection. Such a reflection is then the product of a half-turn (a rotation of order 2) and I , hence, the number of reflections in the extended group is the number of half-turns in G (case a) or the number of half-turns in the complement $G' - G$ (case b).

The remaining number is that of the rotatory reflections (see Table 6).

Table 5

SYMBOL	ORDER
$C_n \times I$	$2n$ ($n=1, 2, \dots$)
$D_n \times I$	$4n$ ($n=2, 3, \dots$) †
$A_4 \times I$	24
$S_4 \times I$	48
$A_5 \times I$	120
$C_{2n}C_n$	$2n$ ($n=1, 2, \dots$)
D_nC_n	$2n$ ($n=1, 2, \dots$) ‡
$D_{2n}D_n$	$4n$ ($n=1, 2, \dots$) §
S_4A_4	24

† $D_1 \cong C_2 \rightarrow D_1 \times I \cong C_2 \times I$

‡ D_1C_1 is generated by one reflection.

§ D_2D_1 has order 4, and is generated by two orthogonal reflections.

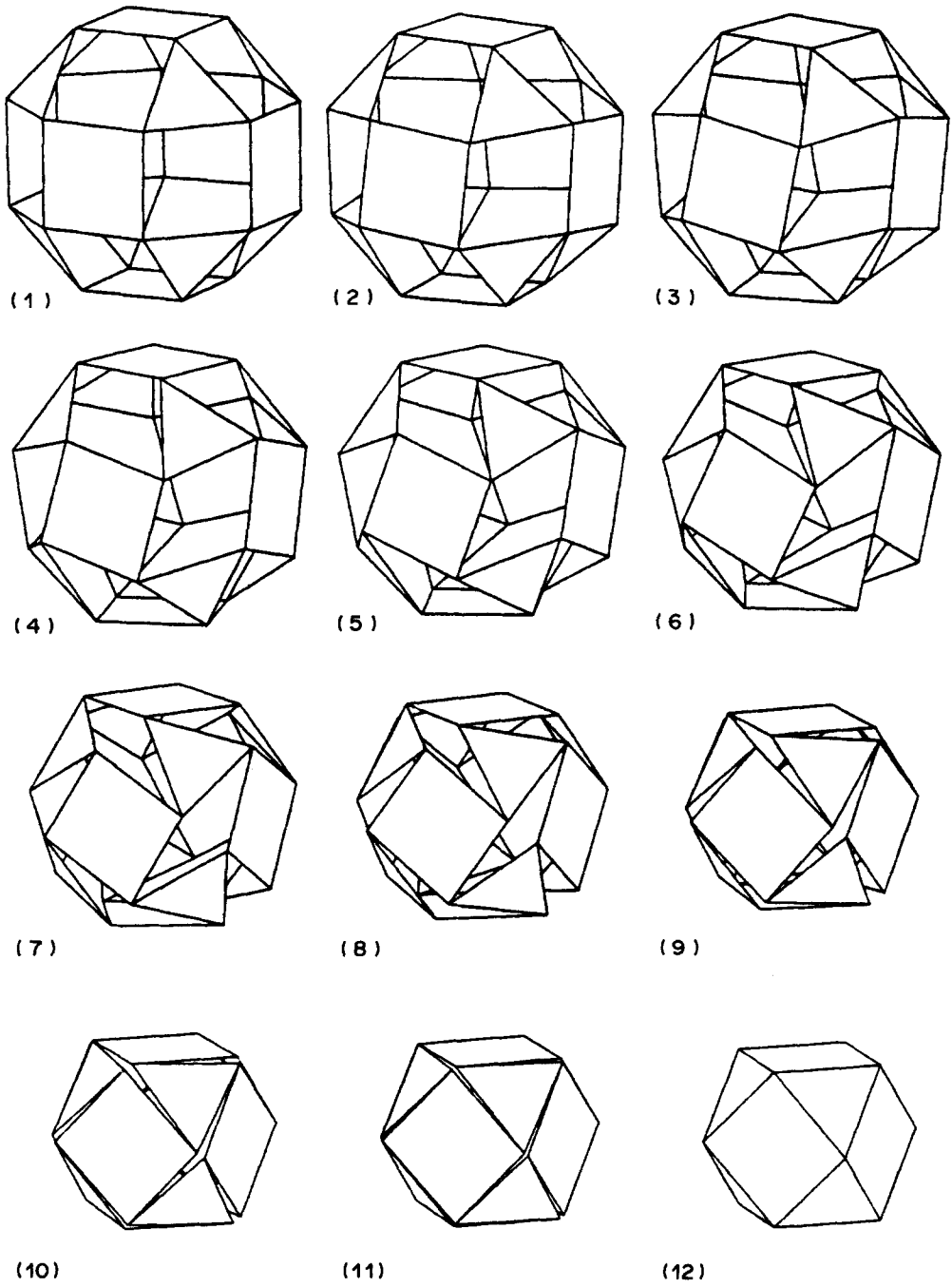


Fig. 16 (1-12)

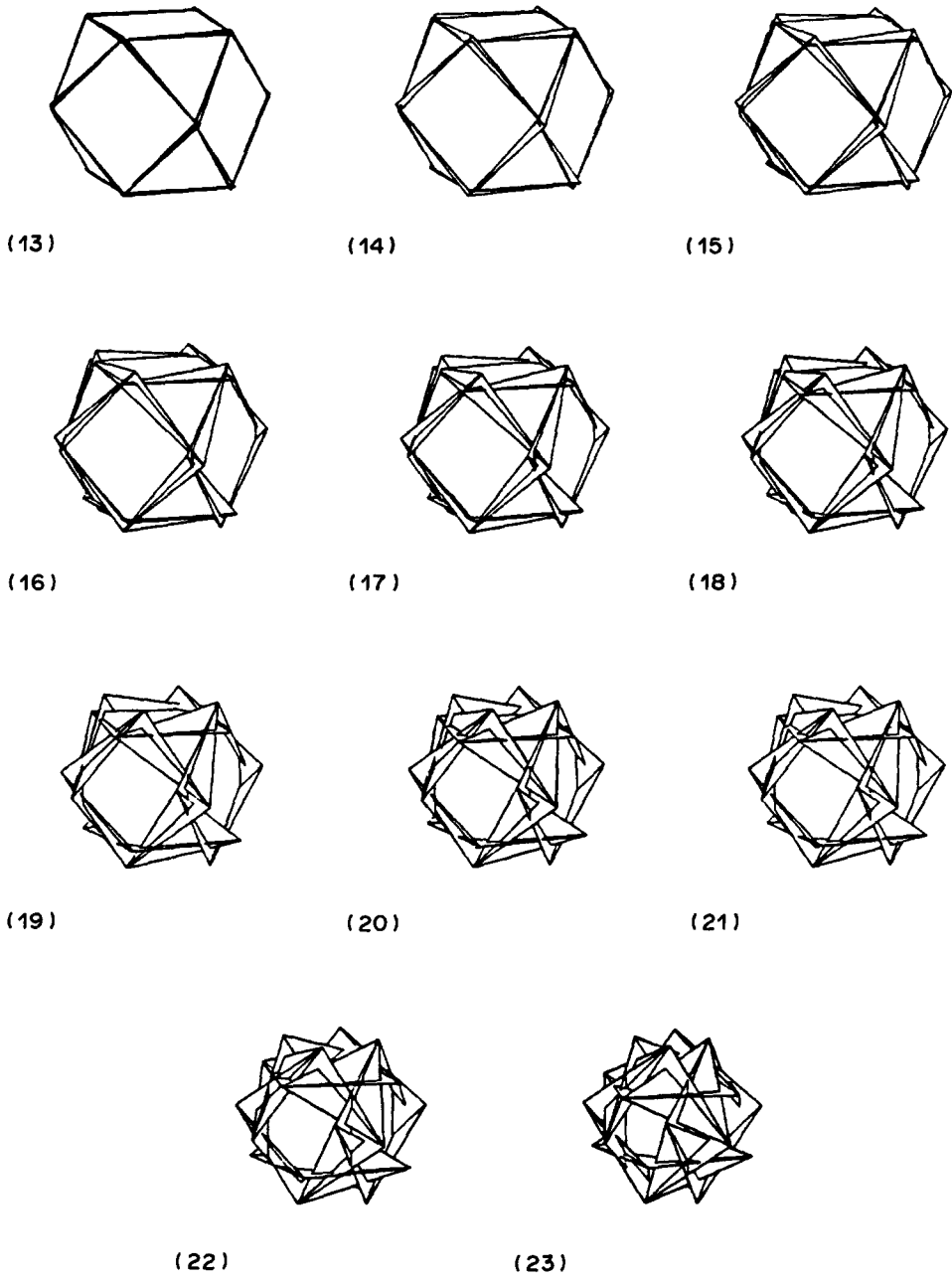


Fig. 16 (13-23)

8.1. Dipolygonal generators

The sets of isometries: $\{A, B\}$; $\{A, B, S\}$; $\{A, B, I\}$, each are called dipolygonal generator sets of symmetry groups. The group

$$F = \text{gen}\{A, B, C\},$$

where $C \in \{S, I\}$, is either discrete, or one of the classified finite groups of isometries containing $G = \text{gen}\{A, B\}$. If F is finite, it contains G as a subgroup of index 2. Then clearly $F = G \cup GC = G \cup CG$.

(1). $C = I$. F is clearly a group of type a , namely a direct product $G \times I$.

(2). $C = S$. The groups in Table 5 have to be checked for their containing of S , with respect to the choice of $\{A, B\}$. This can be obtained from the information given in Table 3, by checking if the two-fold rotation whose axis is perpendicular to ω belongs to G , $G' - G$ or to none of both. It is then also found out whether F is a direct product or a mixed group. From Table 3 also can be seen which axes are perpendicular to the axis of the two-fold rotation, and hence, which are lying in ω . From Table 7 is seen how $D_{2n}D_n$ (n is even) has no dipolygonal generators. It has no reflection plane containing more than one axis, and does not contain I . The results are shown in Table 8.

9. REGULAR DIPOLYGONIDS

In a regular dipolygon (Section 3.2), the polygonal values of A and B , m and n , are equal. The upper half-ellipse of the path lies in α , and v , the intersecting line of α and ω , is along the greater axis of the ellipse.

The reflection V in α is a symmetry operation for the dipolygon in the upper half, since for any P :

$$VB(P) = A(P) \quad \text{or} \quad VB(P) = A^{-1}(P).$$

Table 6

GROUP	ROTATIONS	REFLECTIONS	ROTATORY REFLECTIONS
$C_n \times I$			
n even	n	1	$n-1$
n odd	n	0	n
$C_{2n}C_n$			
n even	n	0	n
n odd	n	1	$n-1$
D_nC_n	n	n	0
$D_n \times I$			
n even	$2n$	$n+1$	$n-1$
n odd	$2n$	n	n
$D_{2n}D_n$			
n even	$2n$	n	n
n odd	$2n$	$n+1$	$n-1$
$A_4 \times I$	12	3	9
S_4A_4	12	6	6
$S_4 \times I$	24	9	15
$A_5 \times I$	60	15	45

Table 7

GROUP	SYMMETRY PLANES	COPLANAR AXES (NUMBER)
$C_n \times I$	0/1	(0)
$C_{2n}C_n$	0/1	(0)
D_nC_n	n	n (1)
$D_n \times I$	n even	2 (n)
	n odd	2 (1), n (1)
	n odd	n (1)
$D_{2n}D_n$	n even	n (1)
	n odd	2 (n)
	n odd	2 (1), n (1)
$A_4 \times I$	3	2 (2)
S_4A_4	6	2 (1), 3 (2)
$S_4 \times I$	3	2 (2), 4 (2)
	6	2 (1), 3 (2), 4 (1)
$A_5 \times I$	15	2 (2), 3 (2), 5 (2)

The choice of A and A^{-1} can be determined such that

$$VB(P) = A(P)$$

Then clearly, V is also a symmetry operation for the dipolygonid being the image of the dipolygon over G . Hence, the dipolygonid is invariant over

$$\text{gen}\{A, B, V\}.$$

Table 8

GROUP	ADDED GENERATOR	EXTENDED GROUP
D_n	S	$D_{2n}D_n$ (n odd) $D_n \times I$ (n even)
	I	$D_n \times I$
A_4	S	S_4A_4
	I	$A_4 \times I$
S_4	S	$S_4 \times I$
	I	$S_4 \times I$
A_5	S	$A_5 \times I$
	I	$A_5 \times I$

Analogue, the reflection W in β is a symmetry operation for the dipolygonid in the lower half, whose symmetry group is then:

$$\text{gen}\{A, B, W\}.$$

To determine these groups of isometries when G is finite, one has to observe if these generated groups contain S and/or I , or none of both.

In the upper half:

$$S \in \text{gen}\{A, B, V\} \Leftrightarrow SV \in \text{gen}\{A, B, V\},$$

SV is the two-fold rotation along v , hence, $SV \in G$. From Table 3 is found if this two-fold rotation is in G . If so, S is a symmetry operation for the dipolygonid, which means it is self-enantiomorphous, and composed of coplanar pairs of polygons $\{m\}$, each along one side at least, of an axis of order s .

The dipolygonid's symmetry group in this half is $\text{gen}\{A, B, S\}$. Analogue, this property occurs in the lower half if, and only if $SW \in G$. Then,

$$SW \in G \Leftrightarrow SVW = I \in \text{gen}\{A, B, S\}.$$

9.1. Conclusions

9.1.1. $\{SV, SW\} \in G$. The symmetry group of the dipolygonid contains S and I . Therefore, it has central inverse symmetry all over the uniform motion, where it is composed of coplanar pairs of polygons $\{m\}$, distributed along both sides of all the s -fold axes of G .

The uniform motion can be analysed when two coplanar pairs forming chiral dipolygons in the upper half are denoted by:

$$\{m\}_1 \text{ and } \{n\}_2/\{m\}_2 \text{ and } \{n\}_1$$

and on the opposite side:

$$\{m\}'_1 \text{ and } \{n\}'_2/\{m\}'_2 \text{ and } \{n\}'_1.$$

When the dipolygonid passes the central position, the polygons $\{m\}$ and $\{m\}'$ reverse their sense of rotation, and keep their sense of translation, while the polygons $\{n\}$ and $\{n\}'$ keep their sense of rotation, but reverse their sense of translation.

In a central position, the following sets of polygons are coplanar:

$$\begin{aligned} &\{\{m\}_1, \{m\}'_1, \{m\}_2, \{m\}'_2\} \\ &\{\{n\}_1, \{n\}'_1, \{n\}_2, \{n\}'_2\}. \end{aligned}$$

Also, continuing over the lower half, the new coplanar pairs become:

$$\{m\}_1 \text{ and } \{n\}'_2/\{m\}'_2 \text{ and } \{n\}_1$$

and opposite:

$$\{m\}'_1 \text{ and } \{n\}_2/\{m\}_2 \text{ and } \{n\}'_1,$$

which actually means the couples "have changed partners".

9.1.2. $SV \in G, SW \notin G$. The dipolygonid's symmetry group in the upper half is $\text{gen}\{A, B, S\}$, which does not contain I , hence, it is a mixed group. The dipolygonid is composed of coplanar pairs of polygons $\{m\}$, distributed along one of both sides of the s -fold axes of G .

The symmetry group in the lower half, $\text{gen}\{A, B, W\}$, may or may not contain I . In any case, the dipolygonid is composed of single polygons $\{m\}$, distributed along both sides of the s -fold axes of G . If I is not within the greater symmetry group, obviously the dipolygonid has no central inverse symmetry. If I is, the dipolygonid's symmetry group is $\text{gen}\{A, B, I\}$.

9.1.3. $SV \notin G, SW \in G$. This is the analogue situation of Section 9.1.2., when upper and lower halves are interchanged.

9.1.4. $SV \notin G, SW \notin G$. The dipolygonid's symmetry groups in upper and lower halves do not contain S and hence, it is composed of single polygons.

When a regular dipolygonid has central inverse symmetry in one of the halves of the path of uniform motion, two opposite polygons rotate in the same sense. If not, provided there are opposite polygons, they rotate in opposite senses.

The uniform motion of the regular dipolygonids in the finite groups of rotations will now be separately analysed. The position of R_A and R_B in ω , together with the axes v and w , provided they belong to G , are shown in Figs 17, 19, 21, 22. These figures are obtained from Tables 3 and 7, and indicate one of the four cases higher described.

9.2. Dihedral

The regular dipolygonids are of the type $n\{2\} + n\{2\} | k/n \cdot 180^\circ$ in D_n , where $n \geq 2$, and $k = 1$ (when $n = 2$), or $1 \leq k < n/2$ where k and n are coprime. These are the Petrie-polygons (non-planar zigzag lines). The bisector line of R_A and R_B in the upper half is v , where the angle between v and R_A is given by:

$$\frac{k}{2n} \cdot 180^\circ$$

According to Table 3, v represents a half-turn of D_n only if $k/2$ is a natural number, specifying to the conditions given there. This will be, when k is even.

The bisector line w in the lower half forms, together with R_A , an angle

$$\frac{n - k}{2n} \cdot 180^\circ$$

and will represent the axis of a two-fold rotation of D_n only when $n - k$ is even.

9.2.1. n is odd, k is odd. Then, $n - k$ is even, referring to case 9.1.3.

Lower half—the symmetry group is $\text{gen}\{A, B, S\} = D_{2n}D_n$ (Table 8). There are n coplanar pairs of digons, each along one side of the n two-fold axes of D_n [Diagram 2(a)].

Upper half—the extended symmetry group not containing S is $D_n \times I$. There are n pairs of centrally inverse digons along each side of the n two-fold axes [Diagram 2(b)].

9.2.2. n is odd, k is even. This refers to case 9.1.2.

The previous situation is found, provided upper and lower halves are interchanged.

9.2.3. n is even. Since k and n are coprime, both k and $n - k$ are odd, which refers to case 9.1.4.

Since the symmetry group must not contain S , and $D_n \times I$ contains both S and I (Table 8), it must be $D_{2n}D_n$ in both halves.

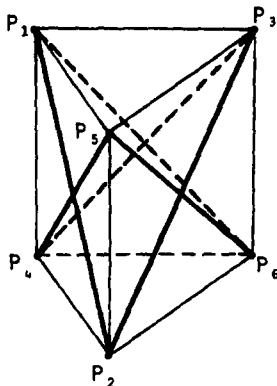


Diagram 2(a). $3\{2\} + 3\{2\} | 60^\circ$ in D_3D_3 : a position in the lower half, described within a triangular prism.

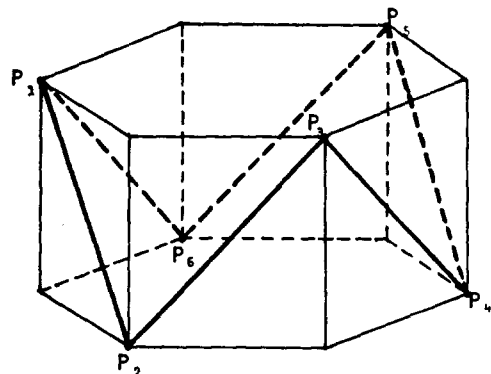


Diagram 2(b). $3\{2\} + 3\{2\} | 60^\circ$ in $D_3 \times I$: a position in the upper half, described within a hexagonal prism.

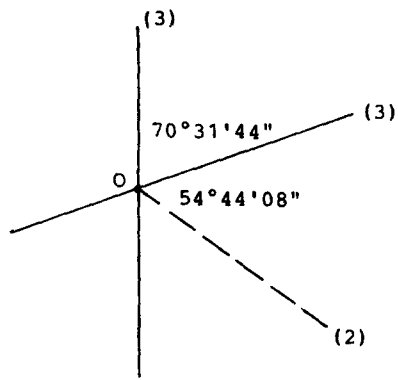


Fig. 17

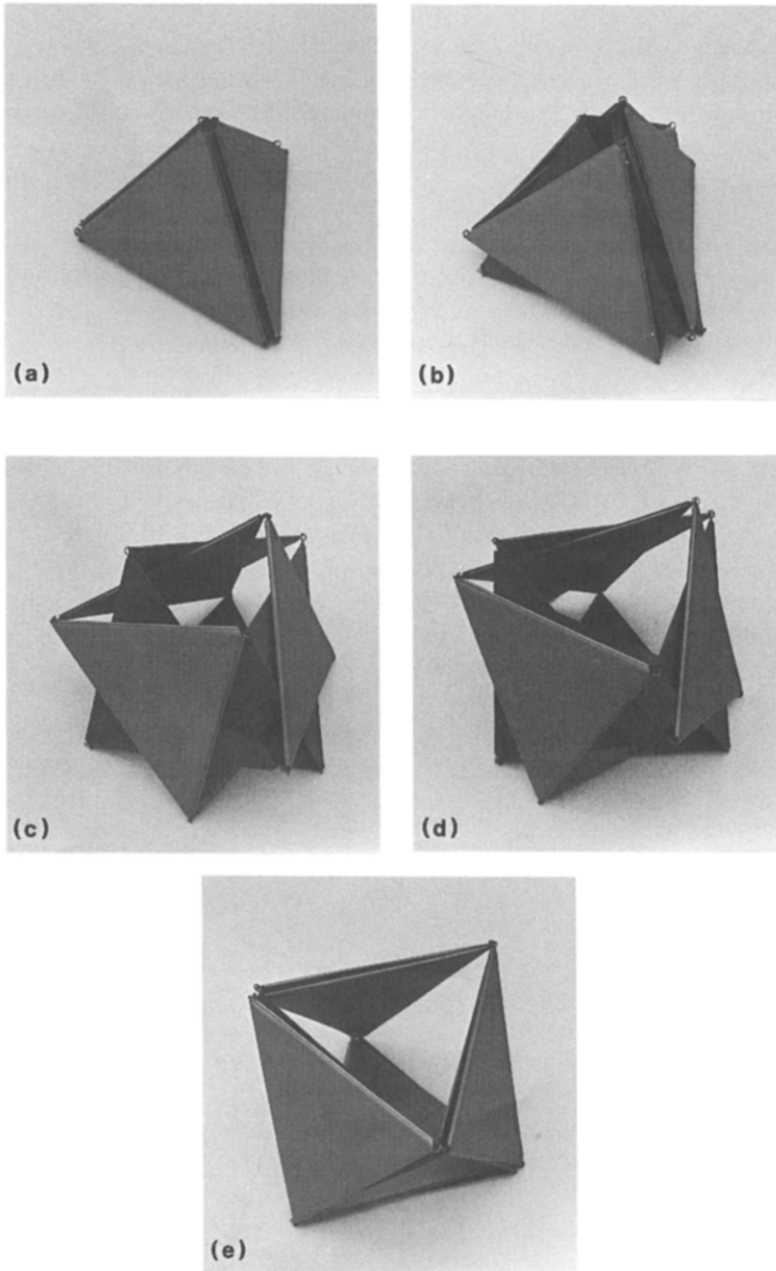


Fig. 18. The convex part of the motion of $4\{3\} + 4\{3\} | 70^\circ 31' 44''$ in S_4A_4 (the lower half) illustrated by a vinyl model in five steps. The minimum position is in (e).

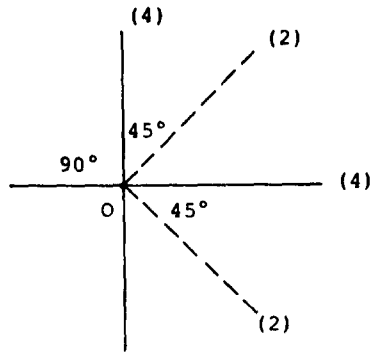


Fig. 19

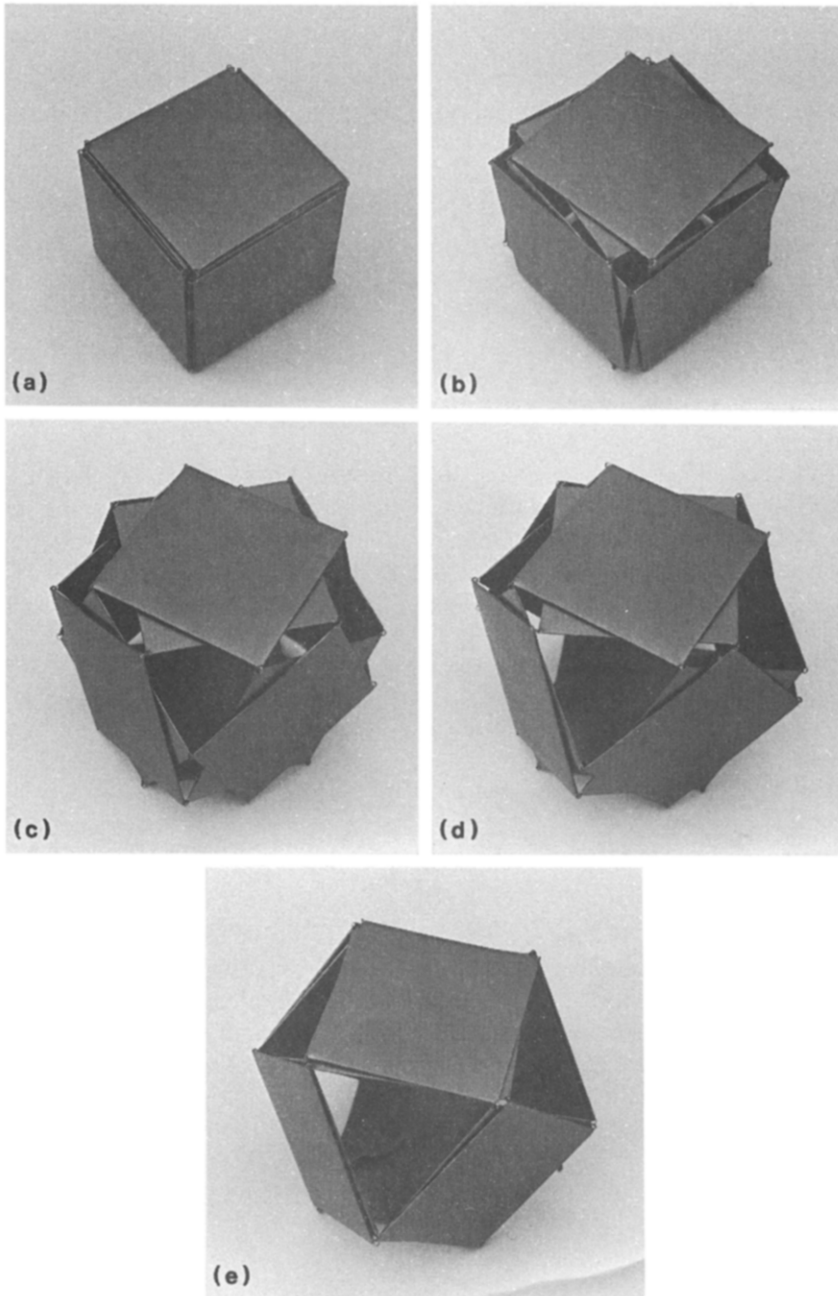


Fig. 20. The convex part of the motion of $6\{4\} + 6\{4\} | 90^\circ$ in $S_4 \times I$, in either lower or upper half, in five steps. The extreme position, illustrated by this cardboard model is in (e).

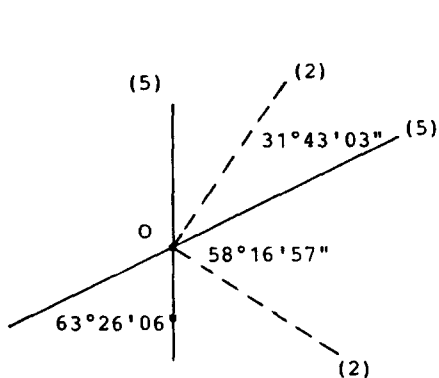


Fig. 21

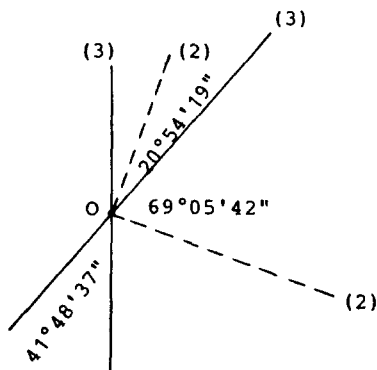


Fig. 22

n pairs of opposite digons appear along both side of the n two-fold axes, each pair being invariant over the half-turn within the cyclic subgroup of order n in D_n .

One peculiar appearance of the regular dihedral dipolygonids occurs in the central positions: since all centers of the $2n$ digons coincide with O , all the digons collapse along the n -fold axis of D_n , as this axis is the intersection of all the planes, perpendicular to the two-fold axes.

9.3. Tetrahedral

The regular dipolygonid in A_4 is of the type

$$4\{3\} + 4\{3\} | 70^\circ 31' 44''.$$

The position of the axes refers to case 9.1.3 (Fig. 17).

Lower half—the symmetry group $\text{gen}\{A, B, S\} = S_4A_4$ (Table 8). There are four coplanar pairs of triangles, each lying along one side of the four three-fold axes of A_4 . (Fig. 18).

Upper half—the extended group not containing S is $A_4 \times I$, which is the dipolygonid's symmetry group. There are four pairs of centrally inverse triangles, each along both sides of the four three-fold axes. The convex part of the uniform motion is Fuller's Jitterbug [Fig. 1(a)].

In the central positions, the four coplanar pairs of triangles have their centers coinciding with O . Such a pair of centrally inverse triangles has its vertices sharing with a regular hexagon. One can picture such a position within the four hexagons found within the cuboctahedron.

The symmetry group in a central position is the direct product of the groups S_4A_4 and $A_4 \times I$, which is $S_4 \times I$, the only group found in Table 5 containing both groups.

9.4. Octahedral

The regular dipolygonid in S_4 is of the type

$$6\{4\} + 6\{4\} | 90^\circ.$$

The position of the axes refers to case 9.1.1 (Fig. 19).

The symmetry group of the dipolygonid containing both S and I (Table 8) is $S_4 \times I$.

In each position there are six coplanar pairs of squares distributed along both sides of the three four-fold axes. The set of squares can also be considered as containing six centrally inverse (hence: parallel) pairs. In a central position, $PO \perp \omega$ and opposite pairs collapse all four with one square. Like explained under case 1, here the "change partners" effect takes place.

The central position can easily be pictured in the location of the three mutually perpendicular squares within the octahedron.

Moreover, since $\theta = 90^\circ$, the positions in upper and lower halves are equivalent (Fig. 20).

9.5. Icosahedral

There are three types of regular dipolygonids in A_5 .

9.5.1. $12\{5\} + 12\{5\} | 63^\circ 26' 06''$. The position of the axes refers to case 9.1.1 (Fig. 21). The symmetry group (Table 8) is $A_5 \times I$.

In each position there are 12 coplanar pairs of pentagons distributed along both sides of the six five-fold axes of A_5 .

Since the half-turn, whose axis is perpendicular to ω , is in A_5 , opposite pairs of pentagons are invariant over this half-turn, as well as over the central inversion. Hence, they are parallel pairs.

In central positions, opposite parallel and centrally inverse pairs coincide with the two pentagons, sharing the 10 vertices of a regular decagon. Here, the "change partners" effect takes place.

A central position can easily be pictured in the location of the six central decagons within an icosidodecahedron.

9.5.2. $12\{5/2\} + 12\{5/2\} | 63^\circ 26' 06''$. The dipolygonid shares its axes with the previous one. Hence, all the results hold when the pentagons are replaced by pentagrams.

9.5.3. $20\{3\} + 20\{3\} | 41^\circ 48' 37''$. The "Vampire".† The position of the axes refers to case 9.1.1 (Fig. 22). The symmetry group is equally $A_5 \times I$.

In each position there are 20 coplanar pairs of triangles distributed along both sides of the 10 three-fold axes of A_5 . For the same reason as in (1) and (2), opposite pairs of triangles are parallel, and centrally inverse. In central positions opposite pairs coincide with two triangles sharing the vertices of a regular hexagon. Also here, the "change partners" effect takes place, when passing that position.

The situation of the triangles can be less easily, but nevertheless correctly, pictured in the location of the 10 central hexagons within the small dodecahemicosahedron [8].

10. EQUIRADIAL DIPOLYGONIDS

Besides the regular dipolygonids of the previous paragraph, for which $R_A = R_B$, there is one more finite equiradial dipolygonid having a particular appearance:

$$12\{5\} + 12\left\{\frac{5}{2}\right\} | 63^\circ 26' 06''.$$

The general dipolygonid of this type, where $R_A \neq R_B$ is composed of opposite pairs of pentagons and pentagrams sharing one five-fold axis. The pentagons and pentagrams are distributed at different distances of O .

However, when $R_A = R_B$, the distances are equal: since the half-turns SV and SW are elements of A_5 , the dipolygonid is composed of 12 coplanar pairs of pentagons–pentagrams. The uniform motion is analogue with the first regular dipolygonid in A_5 (Section 9.5.1), when one pentagon in a pair is replaced by a pentagram.

11. PAIRS OF CHIRAL DIPOLYGONIDS

Pairs of chiral dipolygonids have an extended symmetry group, namely $\text{gen}\{A, B, S\}$. In Section 9 was established where the regular dipolygonids are self-enantiomorphous. The regular dipolygonid of A_4 is so in the lower half, but not in the upper half. A pair of chiral such dipolygonids in the upper half is composed of eight pairs of coplanar triangles distributed along the opposite sides of each of the four three-fold axes, and its symmetry group is the direct product of $A_4 \times I$ and $\{S, E\}$, which, according to Table 5 is $S_4 \times I$. Each chiral pair of dipolygonids is composed of coplanar polygons $\{m\} - \{m\}'$ and $\{n\} - \{n\}'$.

†I built the first model of this dipolygonid in 1979, when I was visiting Magnus J. Wenninger in the Benedictine Monastery in the Bahamas, where I was taught techniques of model making by him. When Wenninger saw the model, he spontaneously baptized it "Verheyen's Vampire" following the tradition among polyhedronists to give horror-names to their weirdest creations. (cf. "Miller's Monster", a complicated non-convex snub polyhedron [3], and "Skilling's Spectre", the Great Disnub Dirhombidodecahedron [10]).

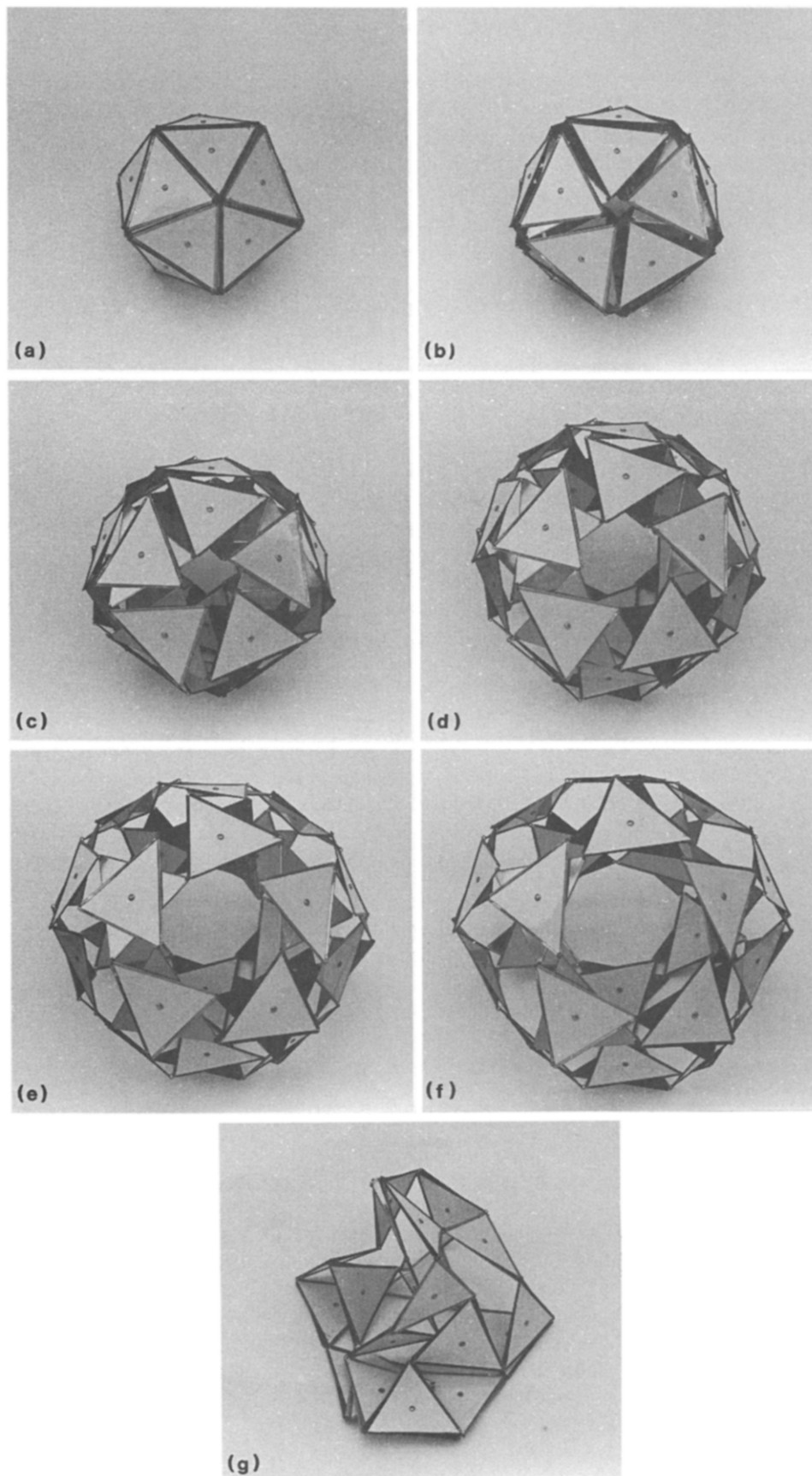


Fig. 23. The convex part of the motion of $20\{3\} + 20\{3\} | 41^\circ 48' 37''$ in $A_5 \times I$ (upper half), illustrated by a metal model in six steps, where (g) had to show the 7th step, namely the maximum position. However, since the proper type of connector (Fig. 24) is replaced here by an ordinary ring, the rigid model loses its rigidity nearing the maximum position, and becomes completely floppy (g).

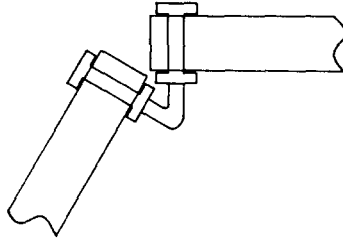


Fig. 24. This type of connector assures the dipolygonal angle θ .

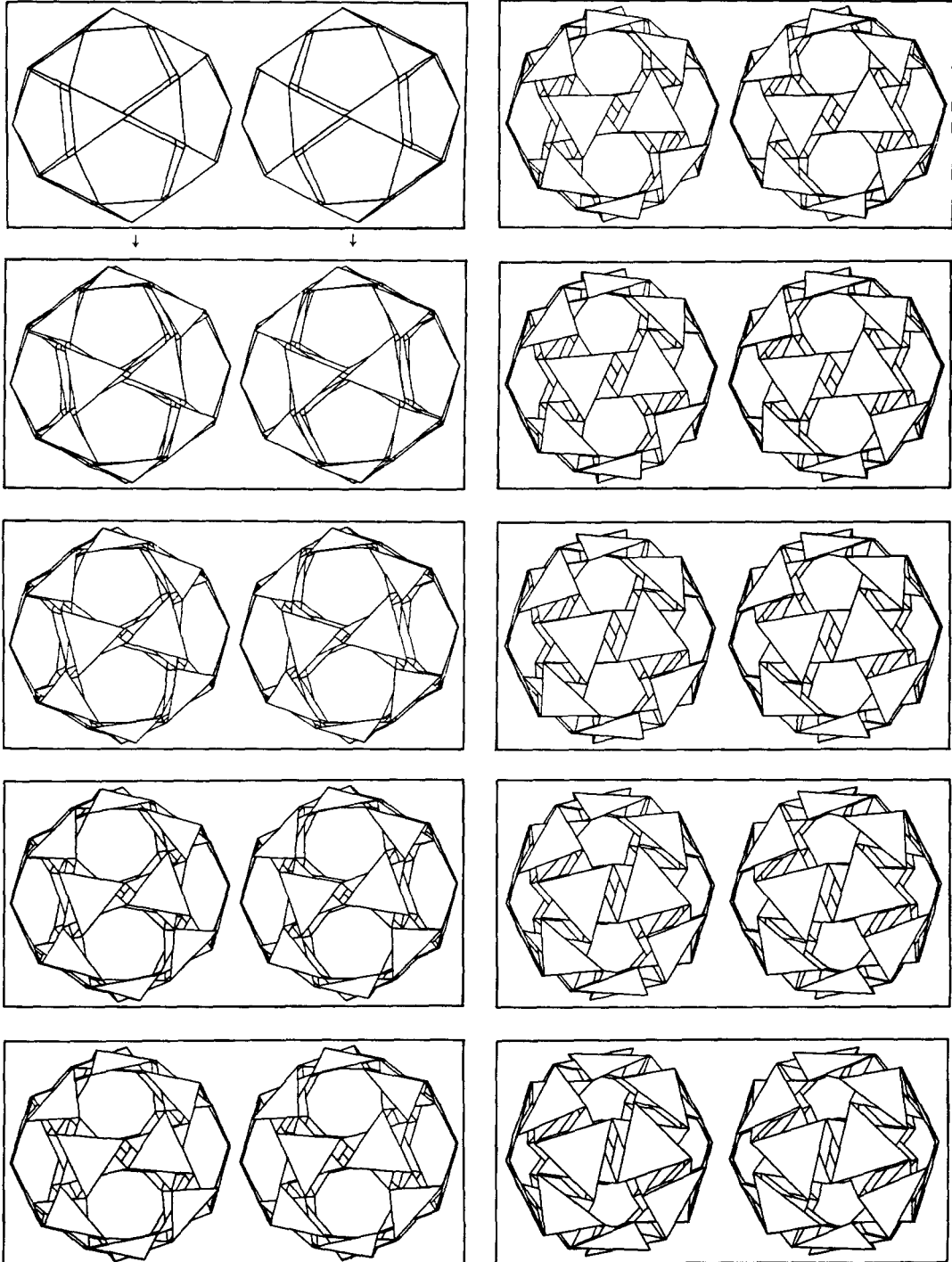


Fig. 25.1.

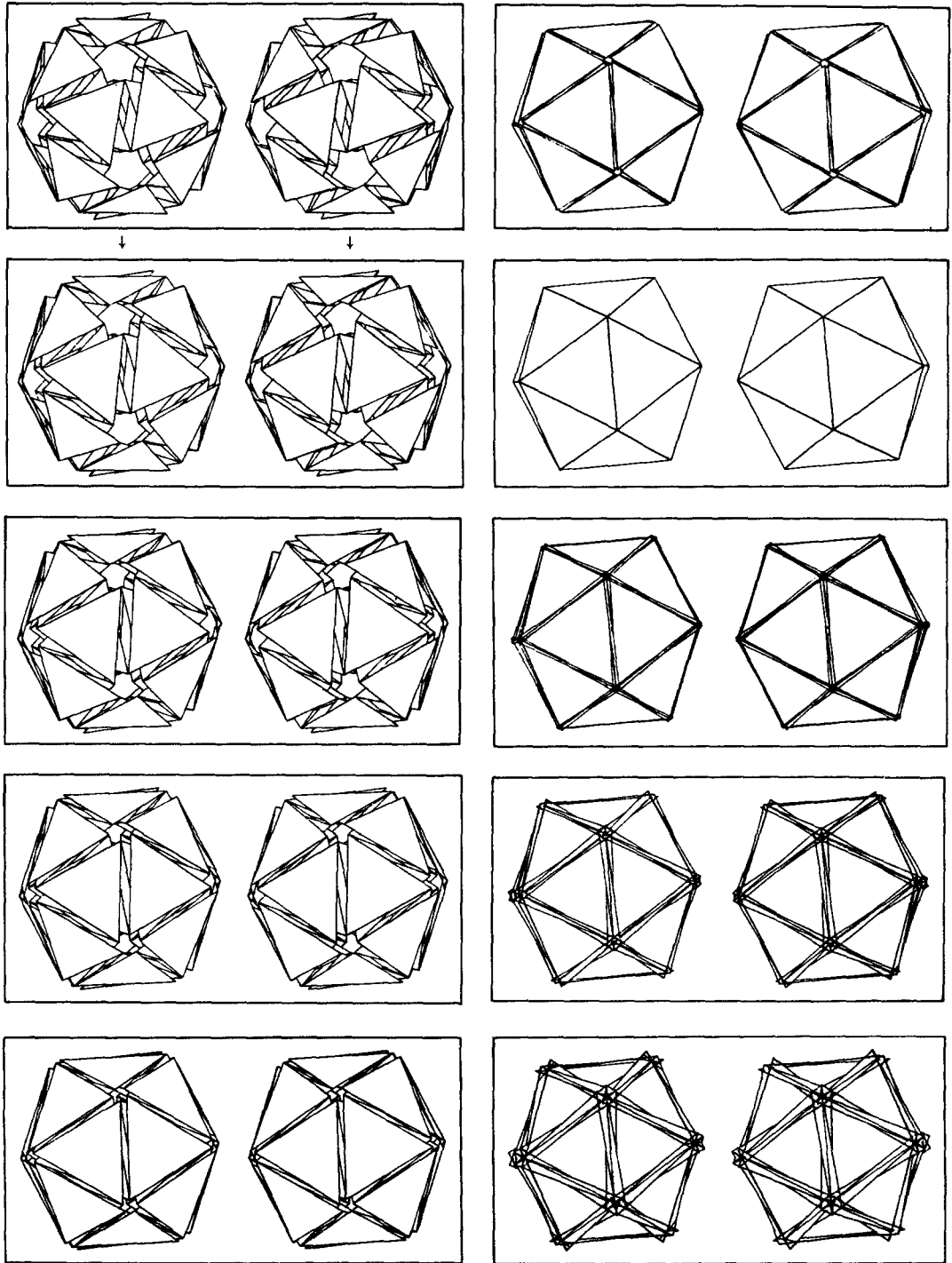


Fig. 25.2.

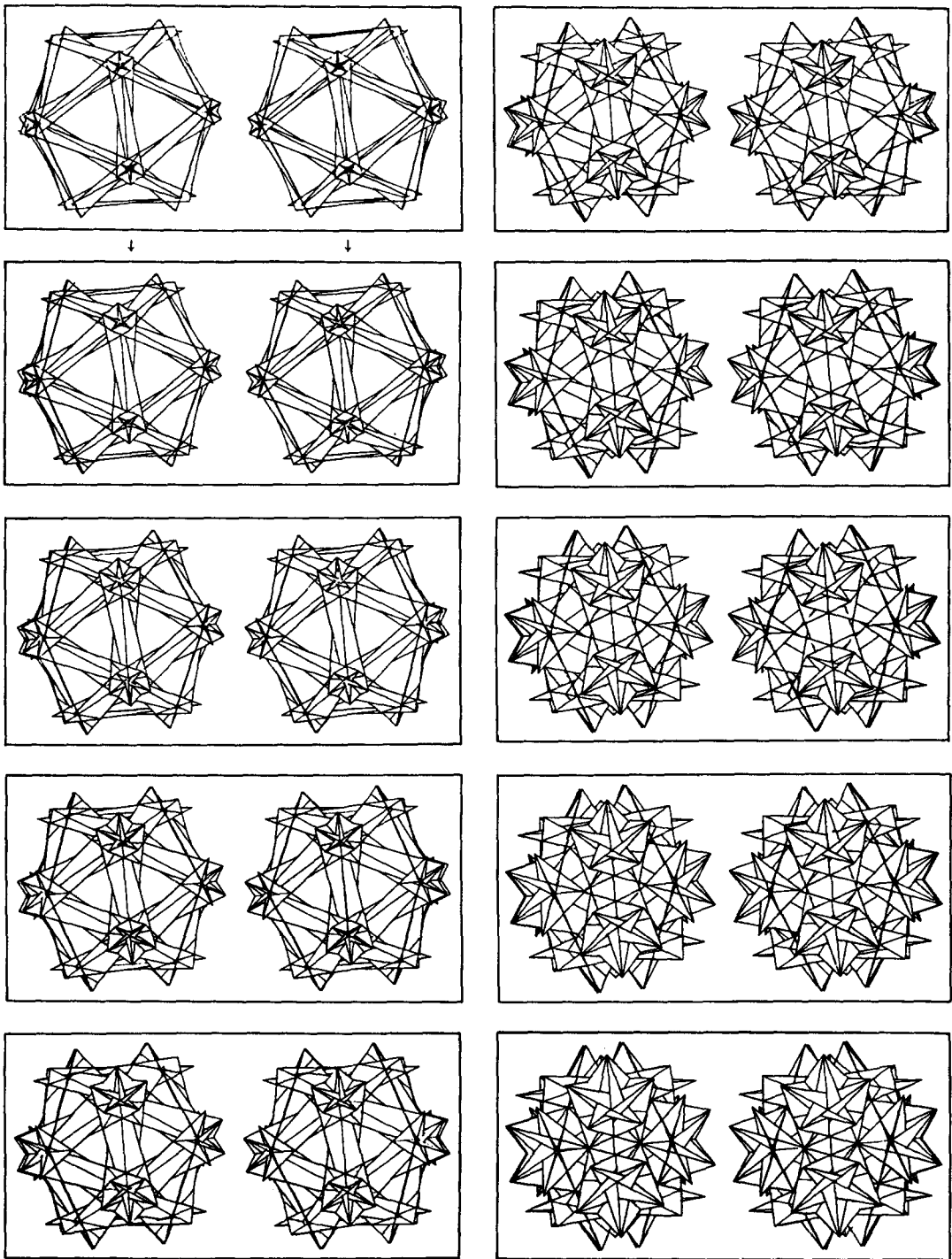


Fig. 25.3.

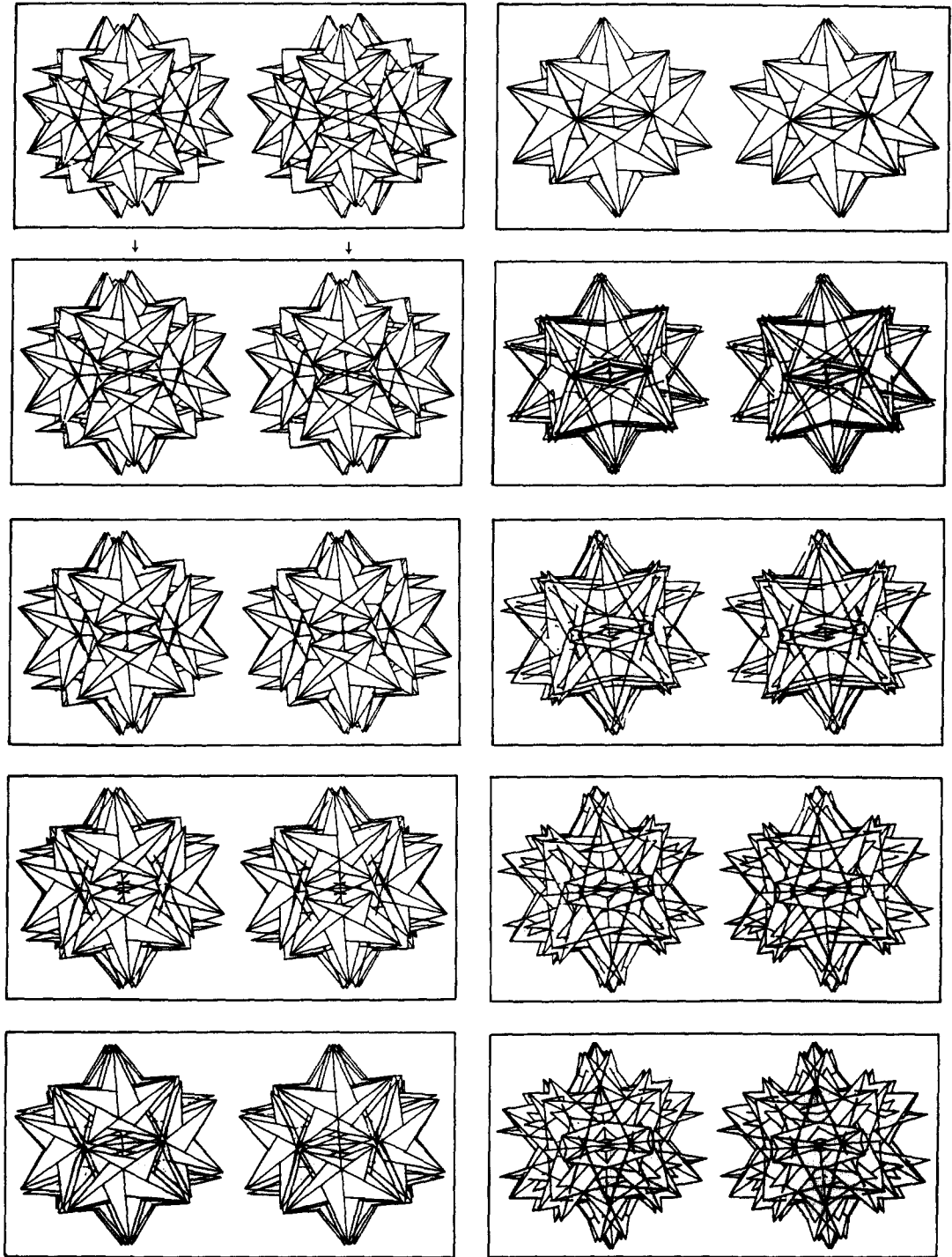


Fig. 25.4.

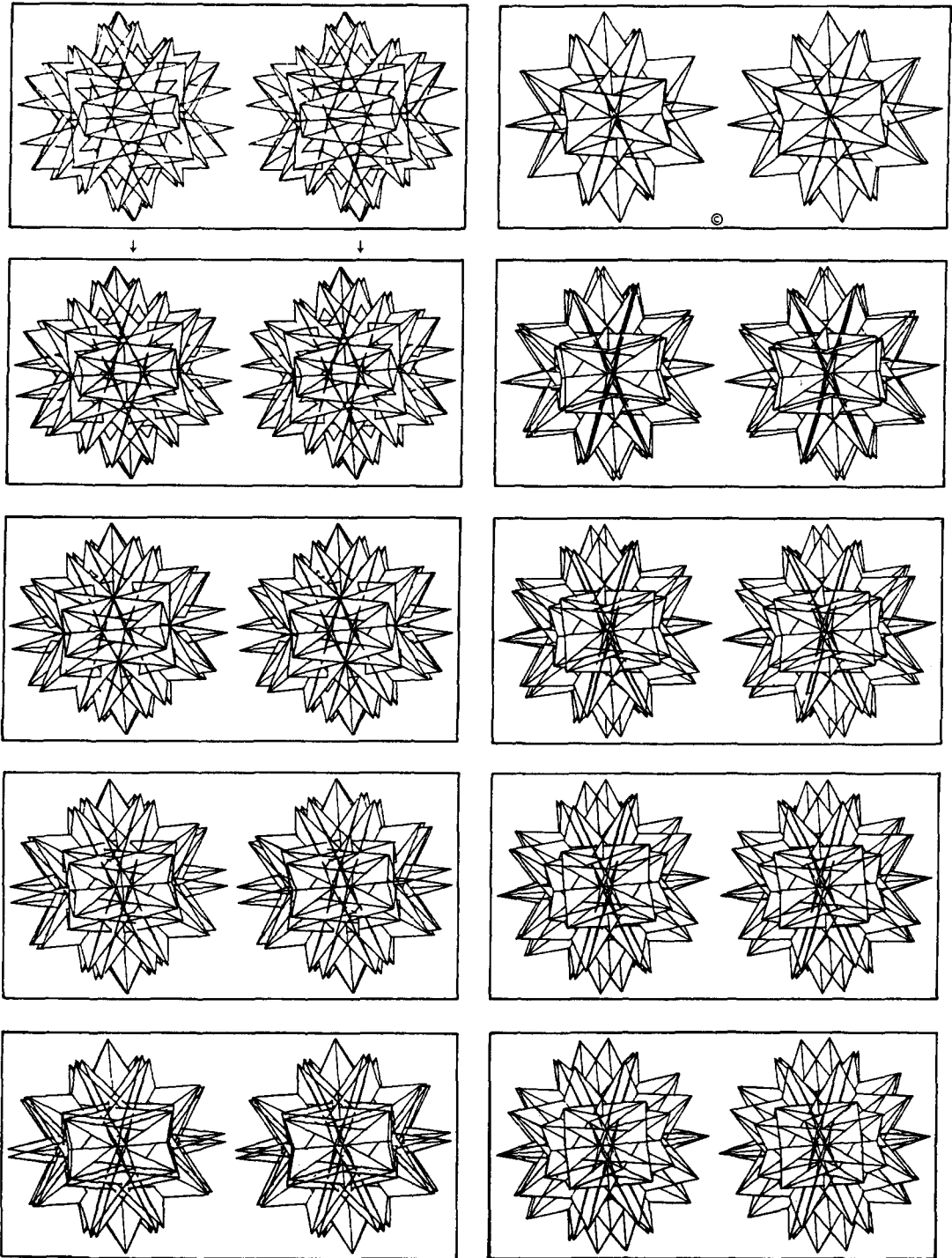


Fig. 25.5.

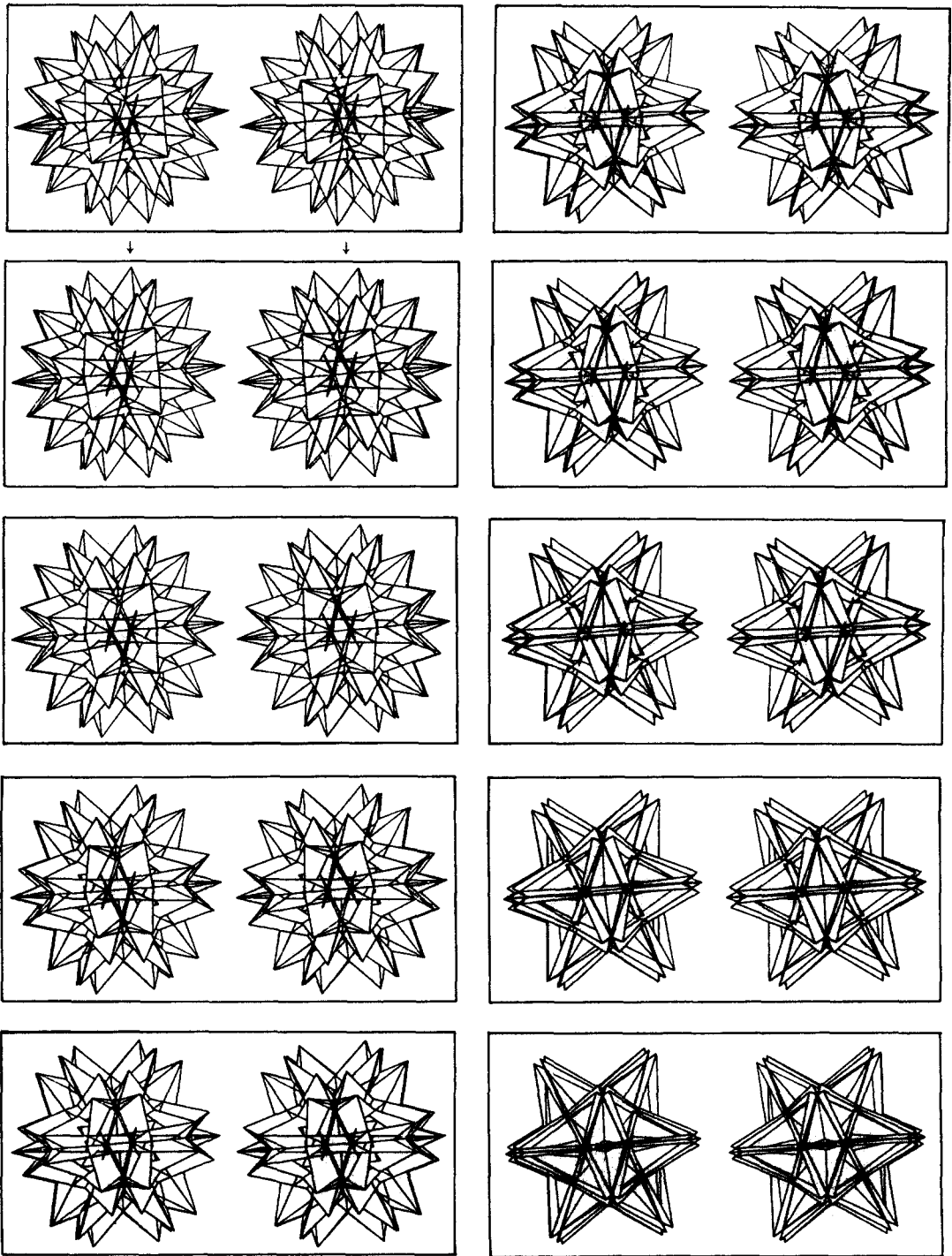


Fig. 25.6.

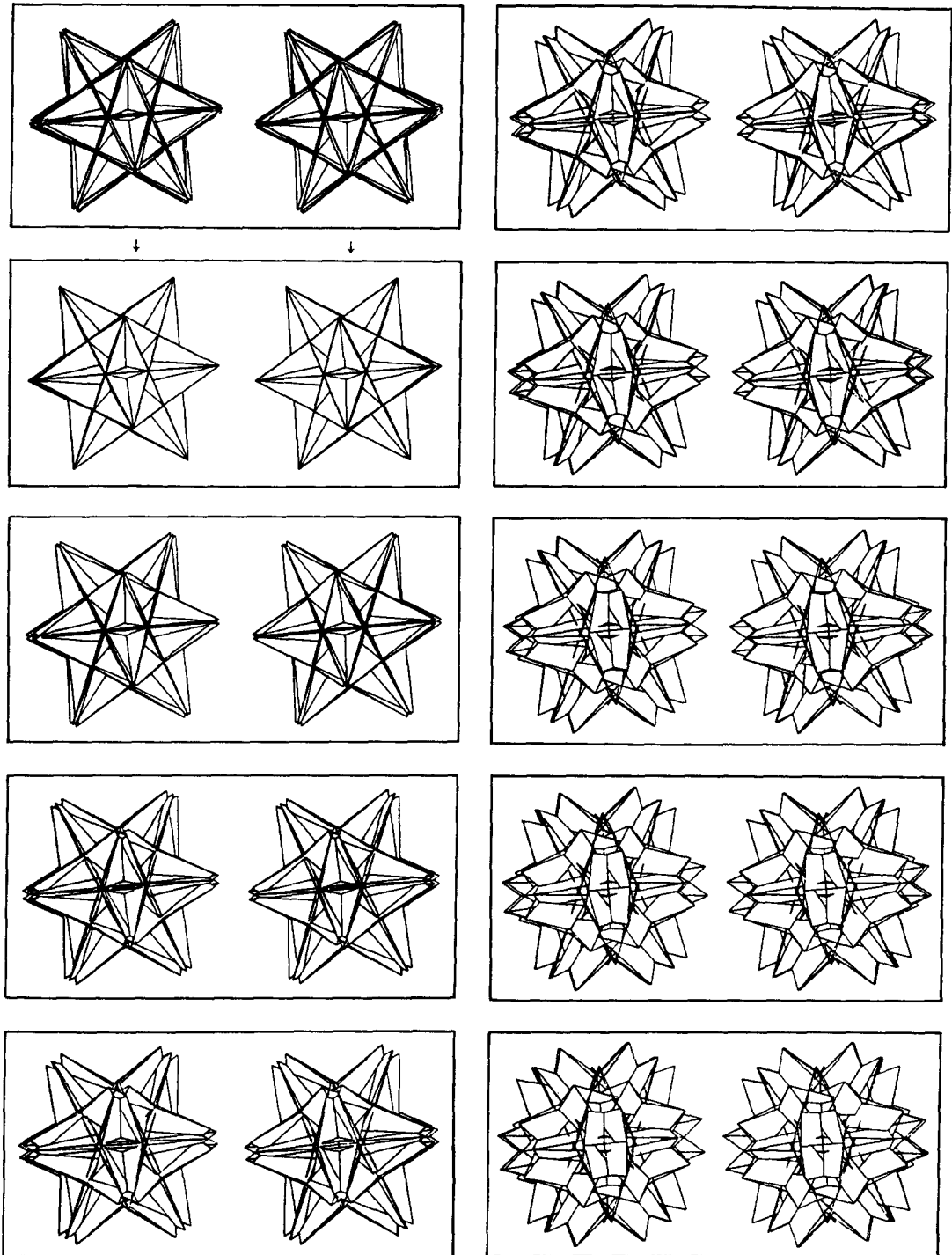


Fig. 25.7.

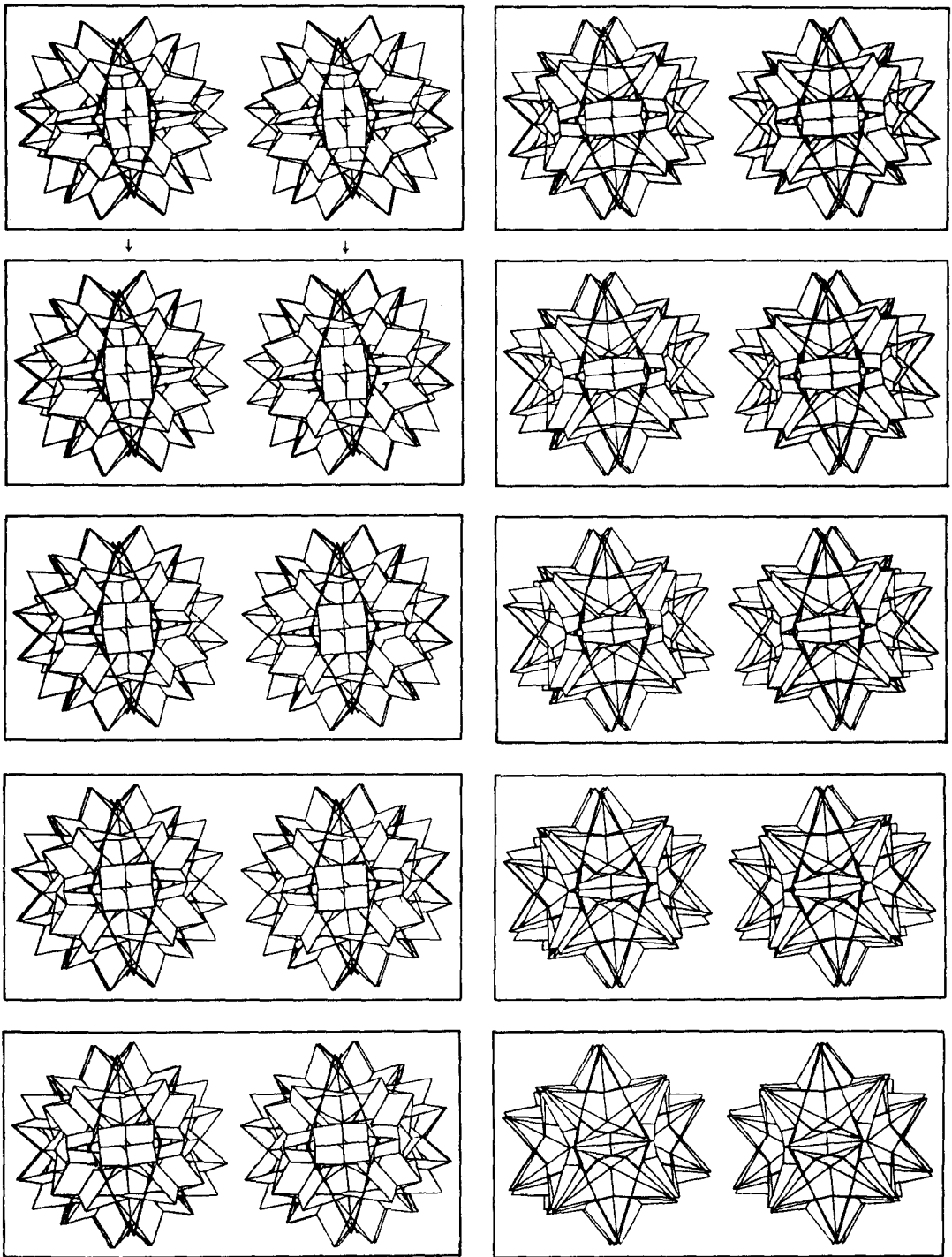


Fig. 25.8.

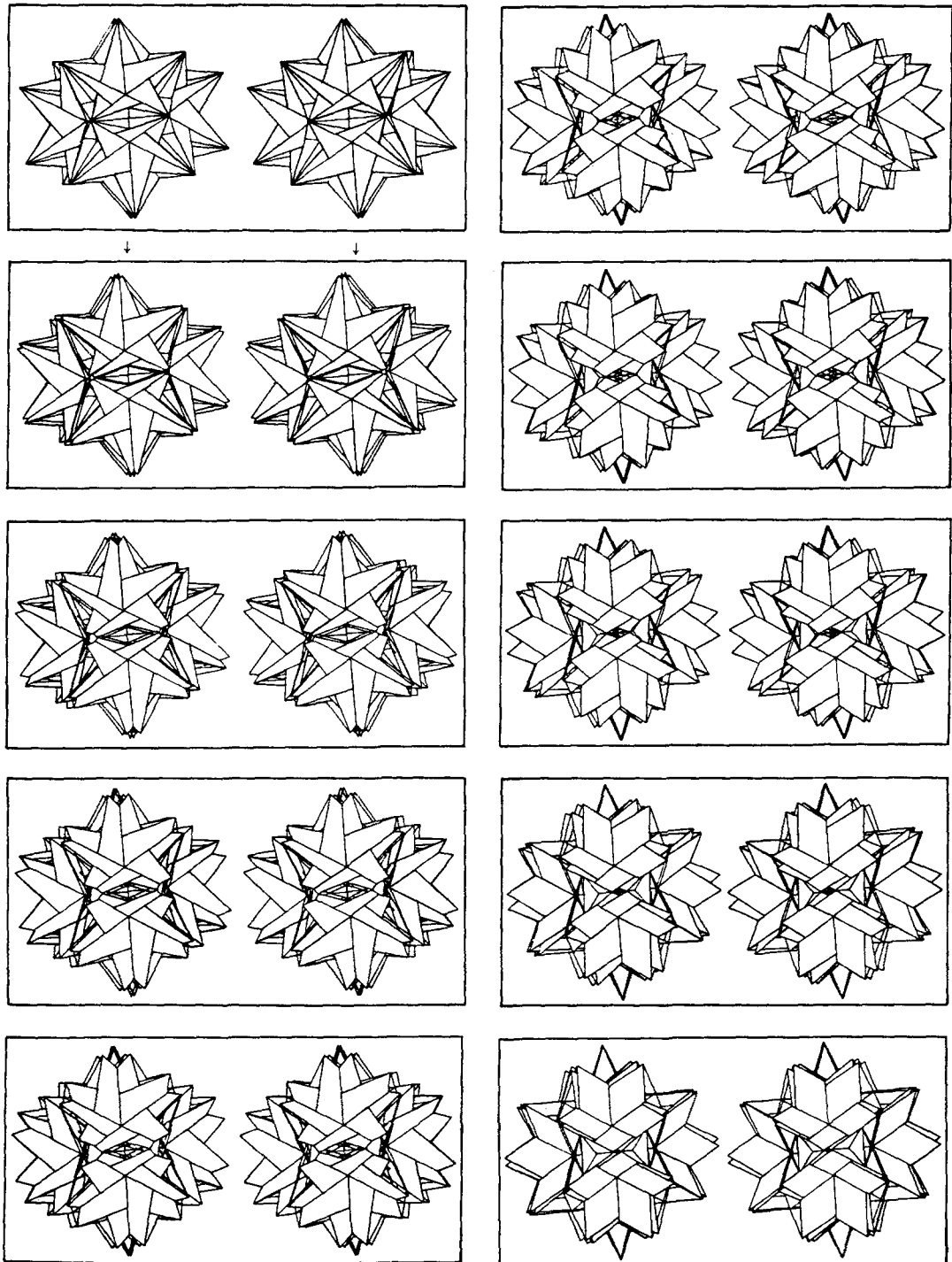


Fig. 25.9.

Fig. 25. Set of stereographic, computer-generated drawings, illustrating the uniform motion of the Vampire from maximum to minimum position. ©: central position.

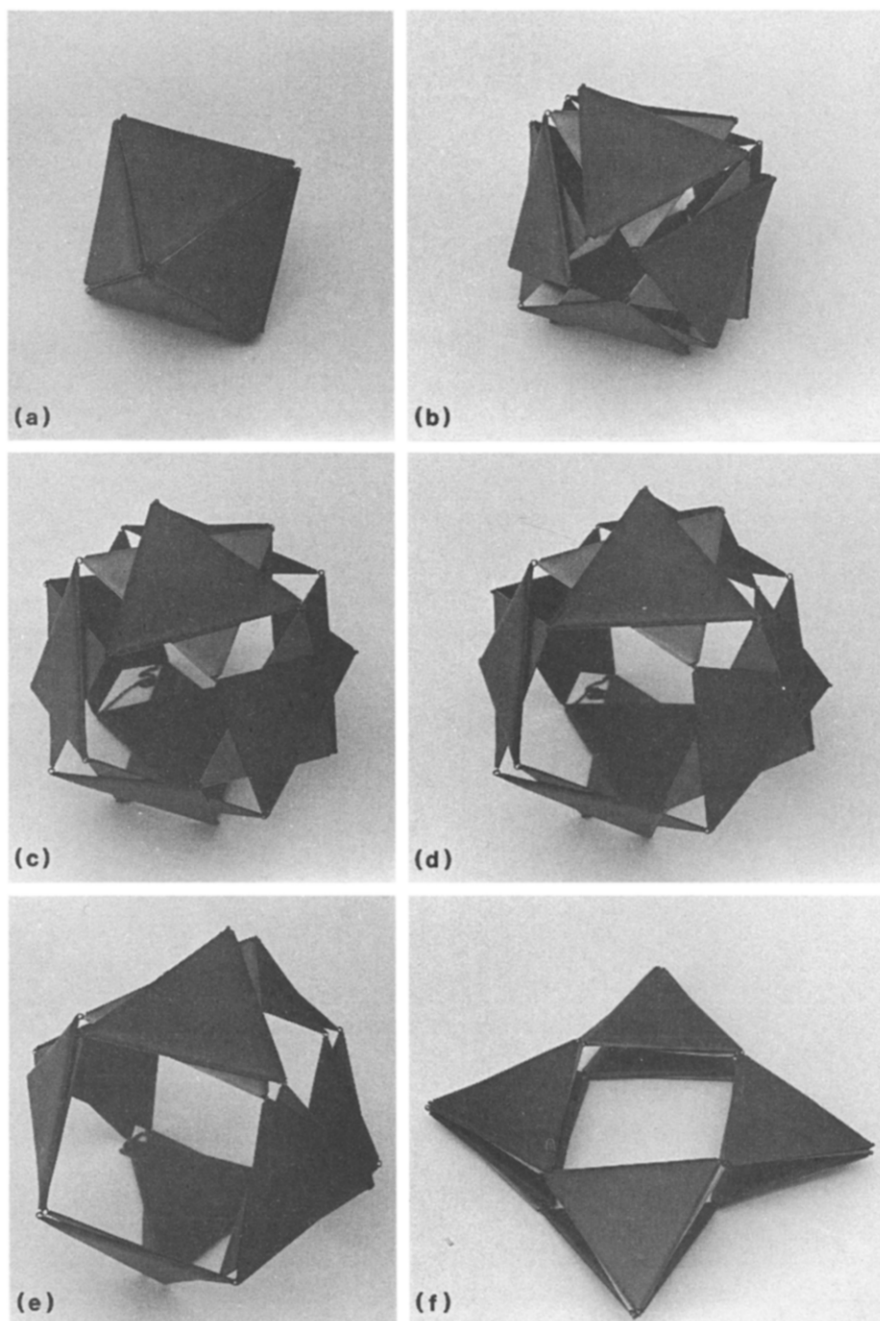


Fig. 26. Motion of a set of two chiral dipolygonids $4\{3\} + 4\{3\} | 70^\circ 31' 44''$ ("Jitterbugs") in $S_4 \times I$, restricted to the convex part, as illustrated here by a vinyl model. As in Fig. 23, the maximum position in (f) is entirely floppy.

As an example, the pair of chiral $8\{3\} + 6\{4\} | 54^\circ 44' 08''$ in $S_4 \times I$ is composed of eight coplanar pairs of triangles and six coplanar pairs of squares. When $R_A = R_B$, clearly there is no "change partners" effect in a central position.

12. THE USE OF DIPOLYGONIDS

The main interest of the dipolygonids is found in an easy to understand visual approach to construct the complete set of uniform polyhedra, in total $75 [3] + 1 [10]$. The details are not within

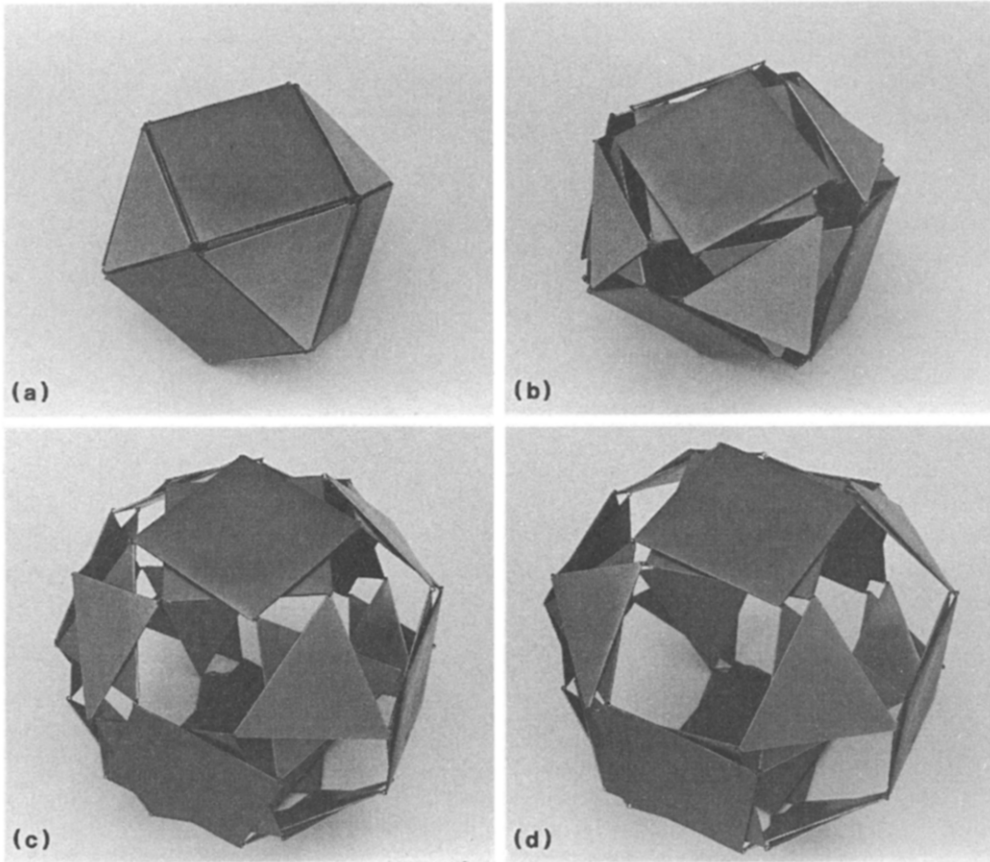


Fig. 27. Model of the two chiral dipolygonids $8\{3\} + 6\{4\} | 54^\circ 44' 08''$ of equal edge length in cardboard. It illustrates the convex part of the uniform motion in the upper half, until it loses the rigidity in the maximum position.

the realm of this paper, however, it can be stated that the convex and non-convex snub polyhedra come out in a natural way during the transformation from one position into another, caused by the uniform motion of triads of dipolygonids (Fig. 28).

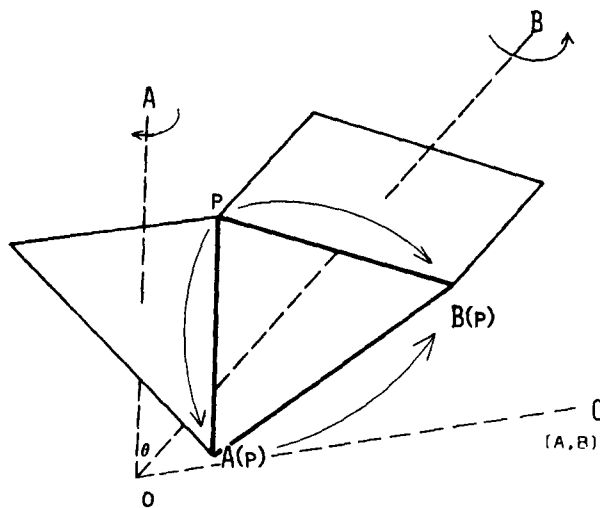


Fig. 28. Triad of dipolygonids. The rotation $C = BA^{-1}$ maps $A(P)$ into $B(P)$ and produces a polygon $\{k\}$.

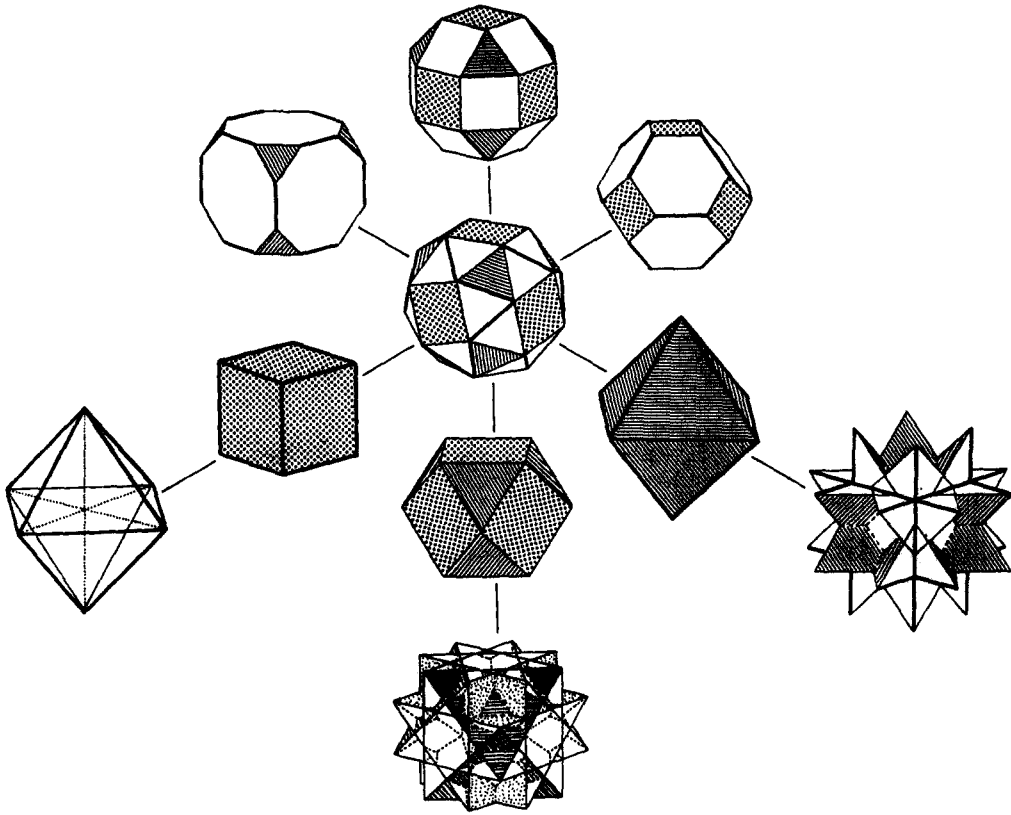


Fig. 29. In the snub cube, three dipolygonids of a basic triad meet.

There can be found 14 basic triads of dipolygonids in A_4 , S_4 and A_5 [6]. In a snub polyhedron, three dipolygonids of a triad meet.

Other applications of dipolygonids can be found in the construction of transformable space frames that are basically space filling lightweight frames, like the impandable edge cube (ICU) and the impandable rhombic edge dodecahedron (IRODO) [11] (Figs 30 and 31).

An example of a spherical variation of an impandable rhombic edge triacontahedron is found at the Space Research Center in Sydney, Australia, where it stands as a reminder of the conference cited in Ref. [12] (Fig. 33).

Dipolygonid models can also be used as space fillers which transform into other space fillers in each position.

Such examples are:

(a) The regular $6\{4\} + 6\{4\} | 90^\circ$ model in $S_4 \times I$, as illustrated in Fig. 20. Twenty-seven of these are used to construct the space filling shown in Fig. 33.

(b) The regular $4\{3\} + 4\{3\} | 70^\circ 31' 44''$ of A_4 , used in:

- (1) the pair of chiral dipolygonids in the upper half, like the model in Fig. 26;
- (2) the dipolygonid in the lower half, like the model in Fig. 18.

When the model (1) shares a pair of triangles of a model (2), the expandable pyramid can be constructed as shown in Fig. 34.

Figure 35 is a variation of the ICU (Fig. 30) when triangular pyramids are replaced by sphere packings. And finally, $6\{4\} + 6\{4\} | 90^\circ$ in $S_4 \times I$ stood model for a piece of furniture, a salon table that is able to transform into a glass and bottle closet, by a push on a button [13], (see Fig. 36).

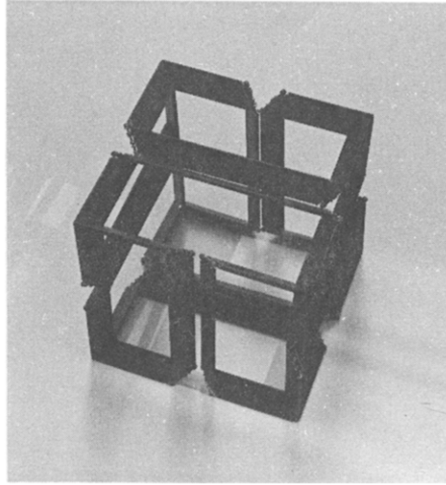


Fig. 30. Model of ICU with wide middle part in wood.

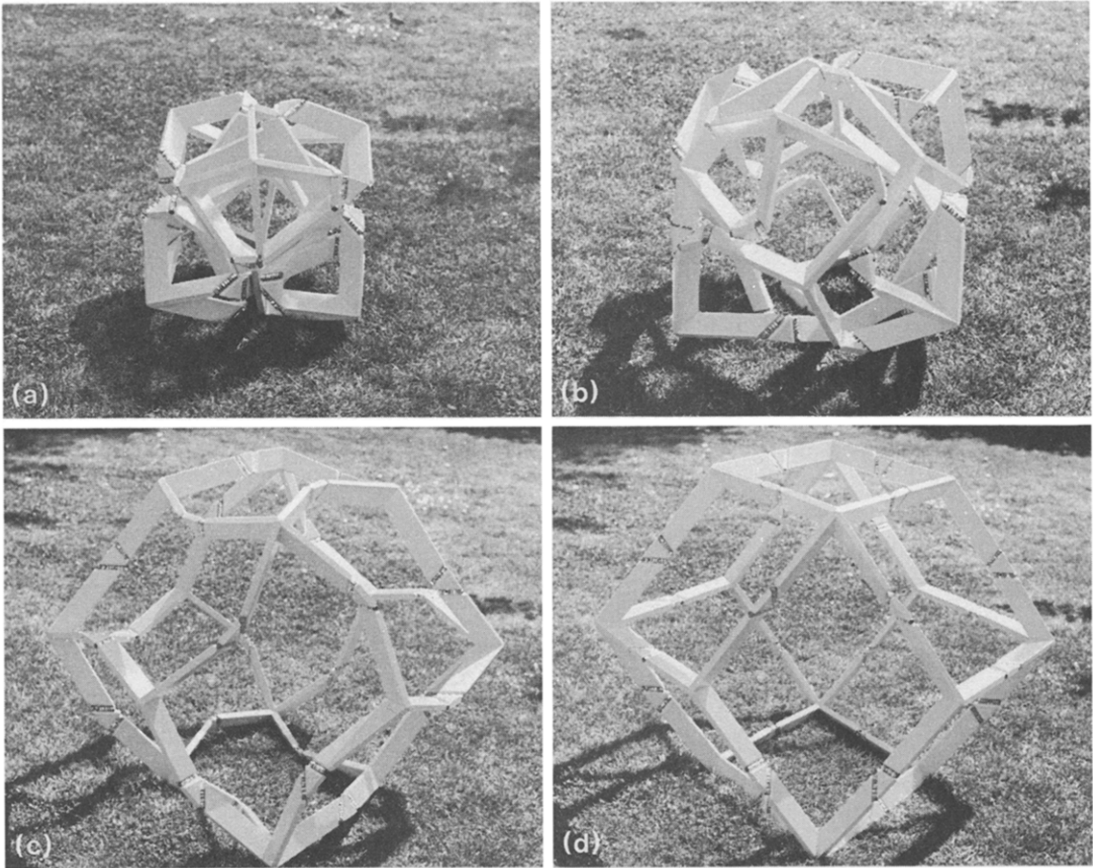


Fig. 31. Impansion of IRODO in four steps. This wooden structure is extremely rigid in all positions.

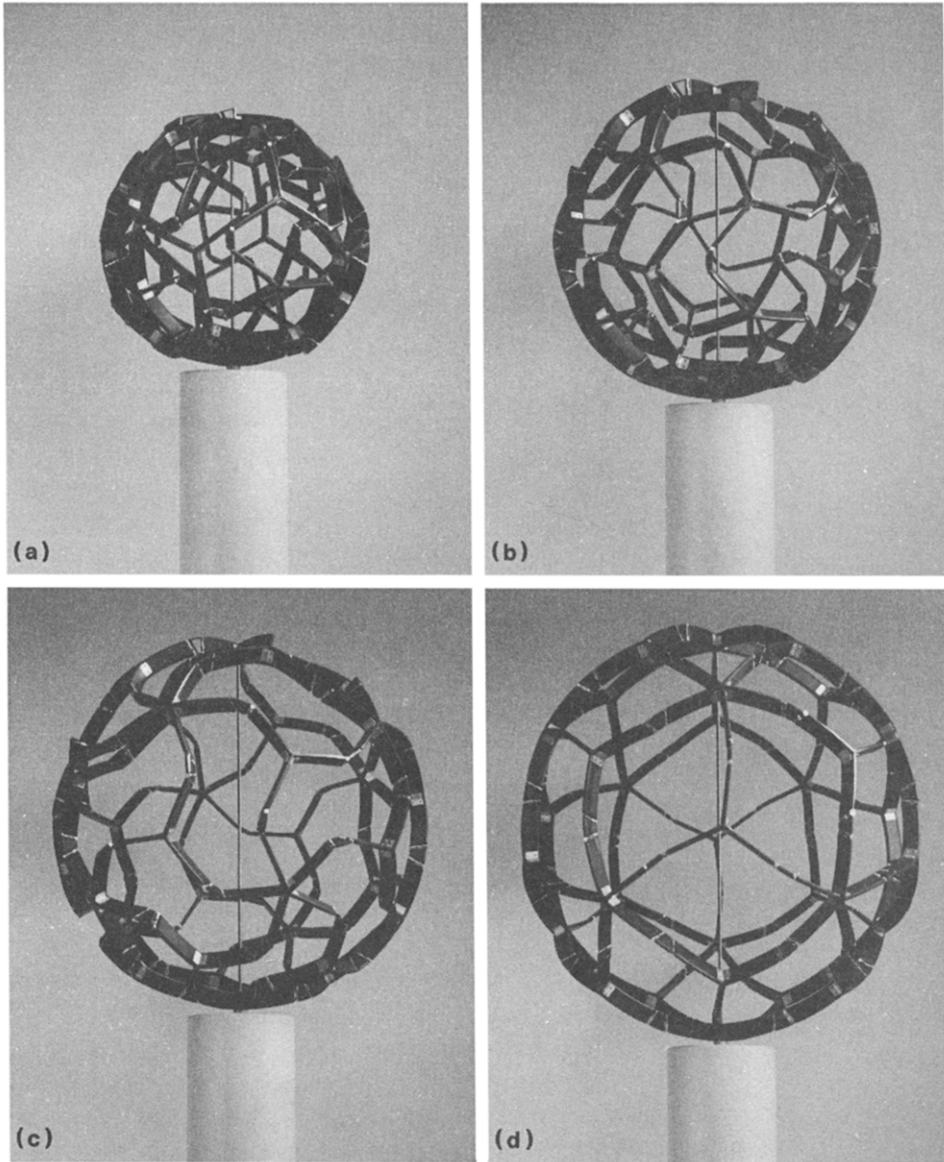


Fig. 32. SPHEROTRAQ in Sydney (University of NSW): motorized model in wood and metal, illustrating a pulsating spherical construction of 120 hinges, rigid in each position.

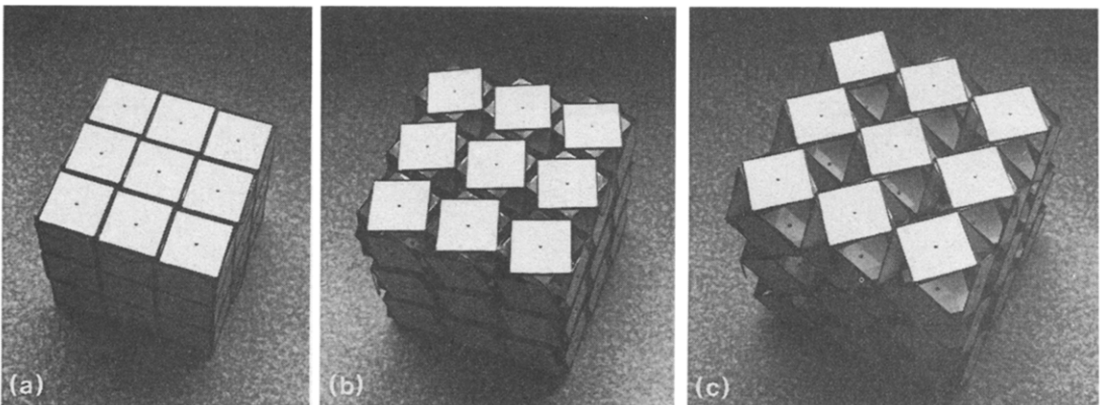


Fig. 33

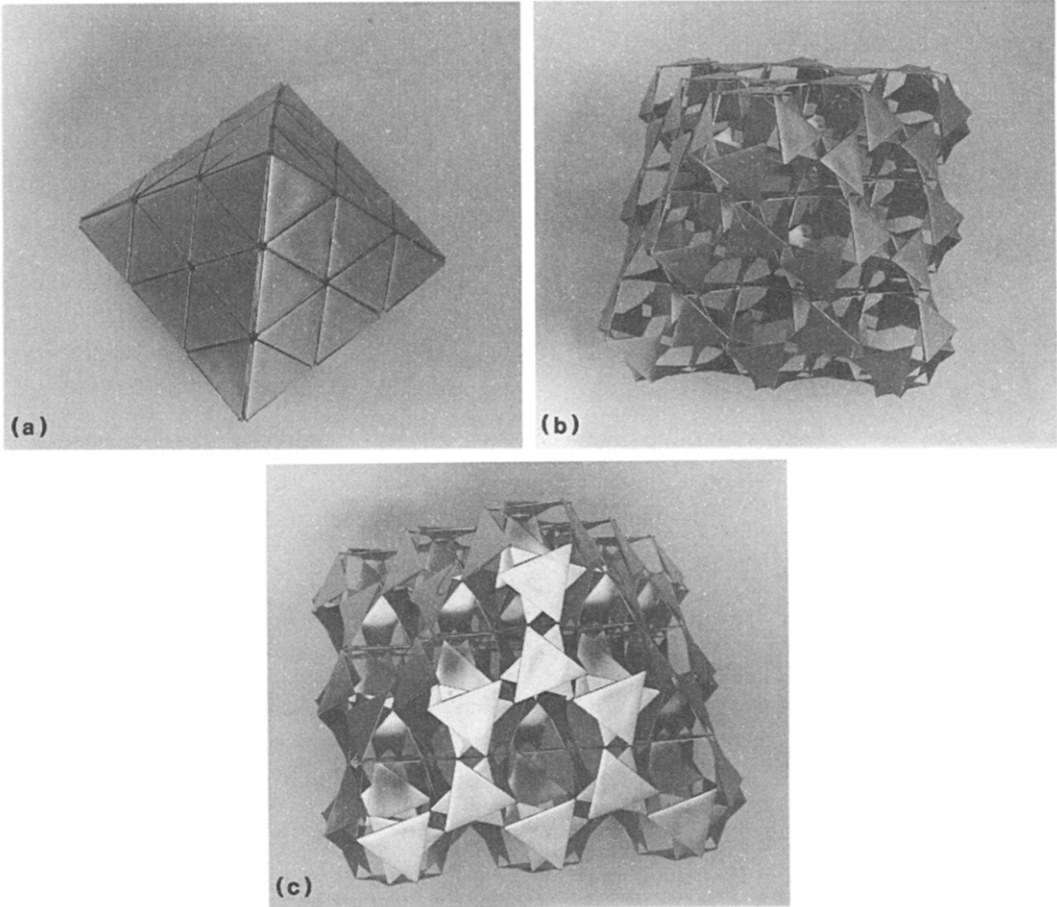


Fig. 34. Expansion of the pyramid in Figs (a) and (b). (c): rotated view of (b).

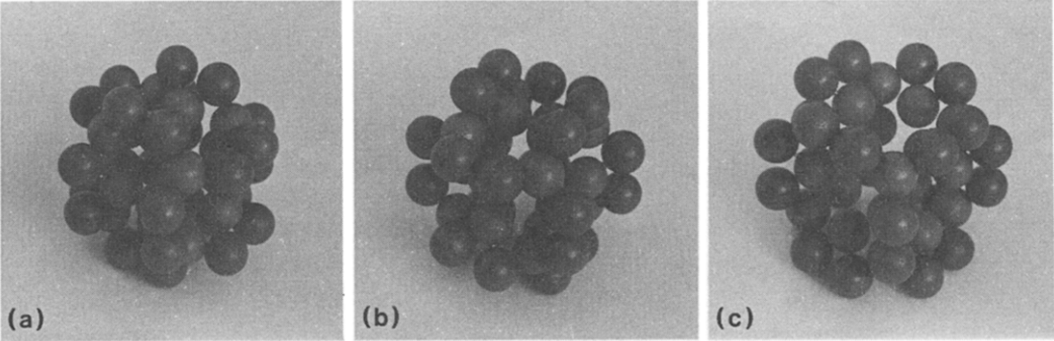


Fig. 35

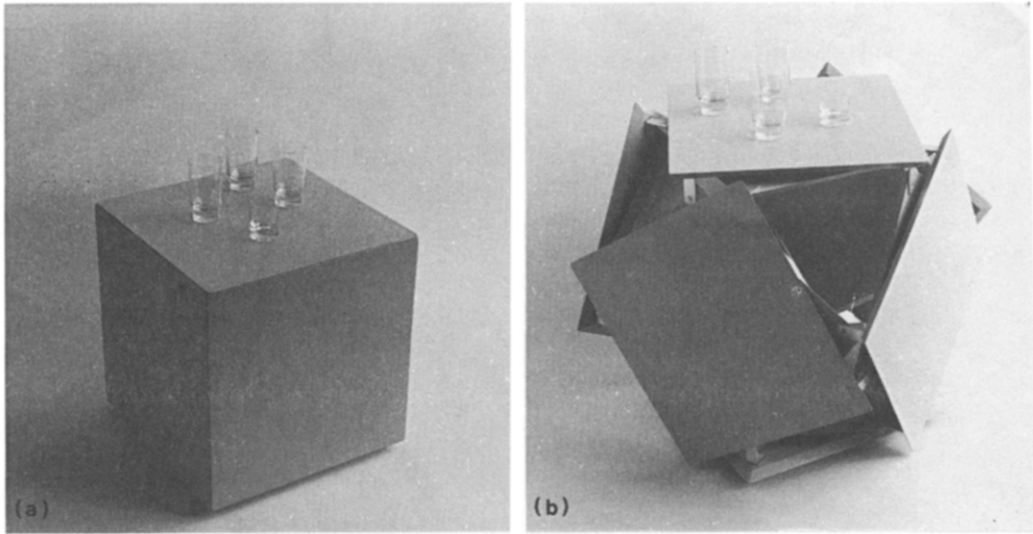


Fig. 36

Acknowledgements—The author wishes to express his gratitude to Dr John Skilling, Department of Applied Mathematics and Theoretical Physics at the University of Cambridge, who developed a special computer program for the uniform motion of dipolygonoids to provide the graphics for Figs 11, 16 and 25.

REFERENCES

1. J. D. Clinton, Advanced structural geometry studies, Part 2. A geometric transformation concept for expanding rigid structures. Southern Ill. Univ., NASA Report CR-1735, Washington D.C. (1971).
2. R. D. Stuart, *Polyhedral and Mosaic Transformations*. Student Publications of the School of Design, Univ. of North Carolina, Vol 12, No. 1 (1963).
3. H. S. M. Coxeter, M. S. Longuet-Higgins and J. C. P. Miller, Uniform polyhedra. *Phil. Trans. R. Soc.* **246A**, 401–450 (1954).
4. B. Grünbaum, Regular polyhedra—old and new. *Equationes Math.* **16**, 1–20 (1977).
5. H. S. M. Coxeter, *Introduction to Geometry*. Wiley, New York (1961).
6. H. F. Verheyen, *Dipolygonoids*. UIA, Univ. of Antwerp, Report 79–40 (1979).
7. H. F. Verheyen, Expandable structures based on dipolygonoids. *Proc. 3rd Int. Conf. Space Structures*. Elsevier, London (1984).
8. M. J. Wenninger, *Polyhedron Models*. Cambridge Univ. Press, New York (1971).
9. F. Klein, *The Icosahedron and the Solution of Equations of the Fifth Degree* (2nd edn). Dover, New York.
10. J. Skilling, The complete set of uniform polyhedra. *Phil. Trans. R. Soc.* **278A**, 111–135 (1975).
11. H. F. Verheyen, Space frames of variable geometry. *Space Structs* **1**, 199–208 (1985).
12. H. F. Verheyen, A pulsating globe. *Proc. 1st Int. Conf. Lightweight Structures in Architecture*. Vol. 1, pp. 476–478. Unisearch, Sydney (1986).
13. H. F. Verheyen, Applications de Géométrie Variable. *Curr. Bois* **78**, 41–44, Brussels (1987).